REPORT DOCUMENTATION PAGE

AD-A200 693

1b. RESTRICTIVE MARKINGS	
3. DISTRIBUTION / AVAILABILITY OF REPORT	
2b. DECLASSIFICATION / DOWNGRADING SCHEDULE	Approved for public release; distribution unlimited.

4. PERFORMING ORGANIZATION REPORT NUMBER(S)

5. MONITORING ORGANIZATION REPORT NUMBER(S)

ARO 21775.4-MS-H

6a. NAME OF PERFORMING ORGANIZATION	6b. OFFICE SYMBOL (If applicable)	7a. NAME OF MONITORING ORGANIZATION
Department of Electrical Engineering		U. S. Army Research Office

6c. ADDRESS (City, State, and ZIP Code)	7b. ADDRESS (City, State, and ZIP Code)
North Carolina A&T State University Greensboro, N.C. 27411	P. O. Box 12211 Research Triangle Park, NC 27709-2211

8a. NAME OF FUNDING / SPONSORING ORGANIZATION	8b. OFFICE SYMBOL (If applicable)	9. PROCUREMENT INSTRUMENT IDENTIFICATION NUMBER
U. S. Army Research Office		DAAG29-84-G-0003

8c. ADDRESS (City, State, and ZIP Code)

P. O. Box 12211
Research Triangle Park, NC 27709-2211

10. SOURCE OF FUNDING NUMBERS

PROGRAM ELEMENT NO.	PROJECT NO.	TASK NO.	WORK UNIT ACCESSION NO.

11. TITLE (Include Security Classification)

Current Controlled Liquid Phase Epitaxial Growth of InGaAsP   Unclassified

12. PERSONAL AUTHOR(S)

A. Abul-Fadl, and S. Iyer

13a. TYPE OF REPORT	13b. TIME COVERED	14. DATE OF REPORT (Year, Month, Day)	15. PAGE COUNT
Final	FROM 1984 TO 1988	September 23, 1988	59

16. SUPPLEMENTARY NOTATION

The view, opinions and/or findings contained in this report are those of the author(s) and should not be construed as an official Department of the Army position, policy, or decision, unless so designated by other documentation.

17. COSATI CODES			18. SUBJECT TERMS (Continue on reverse if necessary and identify by block number)
FIELD	GROUP	SUB-GROUP	Current Controlled LPE or Electroepitaxy, III-V Semiconductor Compounds, Selective Etch-back, Selective Growth, Indium, Gallium Phosphide

19. ABSTRACT (Continue on reverse if necessary and identify by block number) Arsenide Epitaxial Growth, Semiconductor

The current controlled liquid phase epitaxy (CCLPE) or electroepitaxy growth technique has been successfully employed for the first time to grow lattice matched $In_{1-x}Ga_xAs_yP_{1-y}$ quaternary layers of compositions corresponding to wavelengths of 1.31 μm and 1.52 μm. The layers were grown at a constant temperature of 647°C and 685°C. The growth rate of the layers grown at 685°C were 3 to 4 times higher than those grown at 647°C. Further, layers thicker than 3-4 μm could not be grown at a lower growth temperature of 647°C. These have been attributed to composition instabilities in the solid system at the growth temperature of 647°C. On increasing the growth temperature to 685°C, thicker layers as high as 20 μm of good crystal quality have been grown.

The growth velocity of the epilayers grown at 685°C is typically 6 μm/hr and showed a liear dependence on current density, which ranged from 5 to 13

20. DISTRIBUTION / AVAILABILITY OF ABSTRACT	21. ABSTRACT SECURITY CLASSIFICATION
☐ UNCLASSIFIED/UNLIMITED ☐ SAME AS RPT. ☐ DTIC USERS	Unclassified

22a. NAME OF RESPONSIBLE INDIVIDUAL	22b. TELEPHONE (Include Area Code)	22c. OFFICE SYMBOL

DD FORM 1473, 84 MAR   83 APR edition may be used until exhausted.   SECURITY CLASSIFICATION OF THIS PAGE
All other editions are obsolete.   UNCLASSIFIED

A/cm^2. These epilayers exhibit n-type conduction with electron concentration of 1×10^{16}/cm^3 and Hall mobilities of 4,400 cm^2/V-sec.

P-type Mn-doped InGaAsP layers with doping levels varying from 8×10^{16}/cm^3 to 4×10^{18}/cm^3 with excellent surface morphology were grown by liquid phase electroepitaxy. The layers were characterized using X-ray diffraction, Hall and photoluminescence techniques at low temperatures (77°K). Analysis of temperature dependence of concentration data allowed the determination of the activation energy of the Mn-dopant level. The activation energy of the Mn acceptor level decreased from 57 meV to 32 meV with increasing hole concentration from 1×10^{17}/cm^3 to 1.2×10^{18}/cm^3.

Selective etch-back of SiO$_2$-masked (100) Fe-doped InP and (100), (111)A, and (111)B n-type GaAs substrates was performed by electroepitaxy. The etch-back of InP and GaAs was done at constant furnace temperatures of 640°C and 800°C, respectively, by passing a direct electric current from the substrate to the melt. The current density used to etch-back InP was 1 to 5 A/cm^2 for periods from 15 to 60 minutes, and to etch-back GaAs were in the ranges of 5 to 17 A/cm^2 and 50 to 394 A/cm^2 for periods from 10 to 60 minutes. Different mask pattern was used in etching InP and GaAs. In either material, uniform etch-back with excellent surface morphology was obtained on small geometries $\geqslant$200 μm. The electroepitaxial etch revealed well defined crystalline planes. The order of magnitude of the etch rate was {100}>{011}>{111}B>{111}A.

InGaAs layers grown on etched-back InP substrates were of excellent surface morphology and thickness uniformity. The side walls of the grown layers were identified as {111} planes. Consequently, a trapezoid-shaped profile whose sides form an angle of 54° 58' with respect to the (100) surface was obtained along either the (011') or the (01'1') cleavage planes.

Accession For

NTIS GRA&I	☑
DTIC TAB	☐
Unannounced	☐
Justification	

By

Distribution/

Availability Codes

Dist	Avail and/or Special
A-1	

Current Controlled Liquid Phase Epitaxial
Growth of InGaAsP

Final Report

A. Abul-Fadl, and S. Iyer

July 1, 1984 - June 30, 1988

U. S. Army Research Office

Contract No. DAAG29-84-G-0003

North Carolina Agricultural & Technical
State University

Department of Electrical Engineering
Greensboro, N.C. 27411

88 10 19 085

TABLE OF CONTENTS

INTRODUCTION

Epitaxial materials have been used extensively in the fabricaion of opto-electronic devices and integrated circuits. Specific material requirements for high performance devices mandate a detailed understanding of the material propeties affected by the epitaxial growth process, especially the physical parameters relating to device performance.

Liquid phase epitaxy (LPE) has been used in applications requiring high purity layers and abrupt junctions from low temperature depositions. improvements in the control of crystal quality of liquid phase epitaxial layers have been made by the use of current controlled LPE (CCLPE also known as electroepitaxy or LPEE) growth technique.

Electroepitaxial growth is obtained when an dc electric curren is applied across the melt-substrate interface in a LPE system. This growth is carried out in a modified LPE growth system and takes place at constant furnace temperature. Electroepitaxy was first applied to the InSb system[1] and more recently to other III-V compounds such as GaAs[2-4], InP[5],GaAIAs[6], InGaAs[7], and InAs[8]. The results have shown that electroepitaxy yields high quality epitaxial layers exhibiting excellent surface morphology and thickness uniformity, high electron mobilities, and fairly constant impurity profiles.

The primary objective of this study was to investigate the growth by electroepitaxy of undoped and doped InGaAsP lattice matched to InP over the entier quaternary composition range in the temperature range of 550 °C to 650 °C. The original objective was later altered to include selective etch-back and growth of InGaAs and selective etch-back of GaAs. The material characterization included: surface morphology and layer uniformity, carrier concentra-

tion and mobility determination, photoluminescence, and X-ray diffraction. The selective etch-back characterization included: etch-back uniformity, dependence of etch-back on substrate orientation, and identification of etch-revealed crystalline planes.

2.1   EXPERIMENTAL APPARATUS AND PROCEDURE

A block diagram of the system used in the electroepitaxial growth of InGaAsP, electroepitaxial etch-back and growth of InGaAs, and electroepitaxial etch-back of GaAs is shown in Fig. 1. The system , as a whole, consists of a three zone transparent furnace controlled by three Eurotherm temperature controllers. A schematic cross section of the horizontal boat assembly used for the growth and etch-back is shown in Fig. 2. The body of the boat was made from high purity, high density graphite parts and pyrolytic boron-nitride pieces. Growth or etch-back occur only when the substrate is brought into contact with the melt and direct electric current is passed across the substrate-melt (S-M) interface for growth and M-S for etch-back. The back contact melt is used to insure uniform electrical contact between the back surface of the substrate and the bottom part of the graphite boat. The pyrolytic boron-nitride pieces are used to provide electrical insulation and to confine the current flow to the S-M interface only

2.2   GROWTH AND CHARACTERIZATION OF InGaAsP

Electroepitaxy has been used successfully to grow the quaternary alloy. InGaAsP quaternary alloys of energy gap corresponding to a wavelength of 1.31 μm and 1.52 μm have been studied in detail. These alloys have applications in devices for optical fiber communications since the fibers exhibit desirable transmission and dispersion properties in these wavelength regions.

In a typical run the growth melt consisted of 6N pure In (4-5 grams). The weights of other components were based on the liquidus composition of the quaternary melt as reported by Hsieh[9].

tion and mobility determination, photoluminescence, and X-ray diffraction. The selective etch-back characterization included: etch-back uniformity, dependence of etch-back on substrate orientation, and identification of etch-revealed crystalline planes.
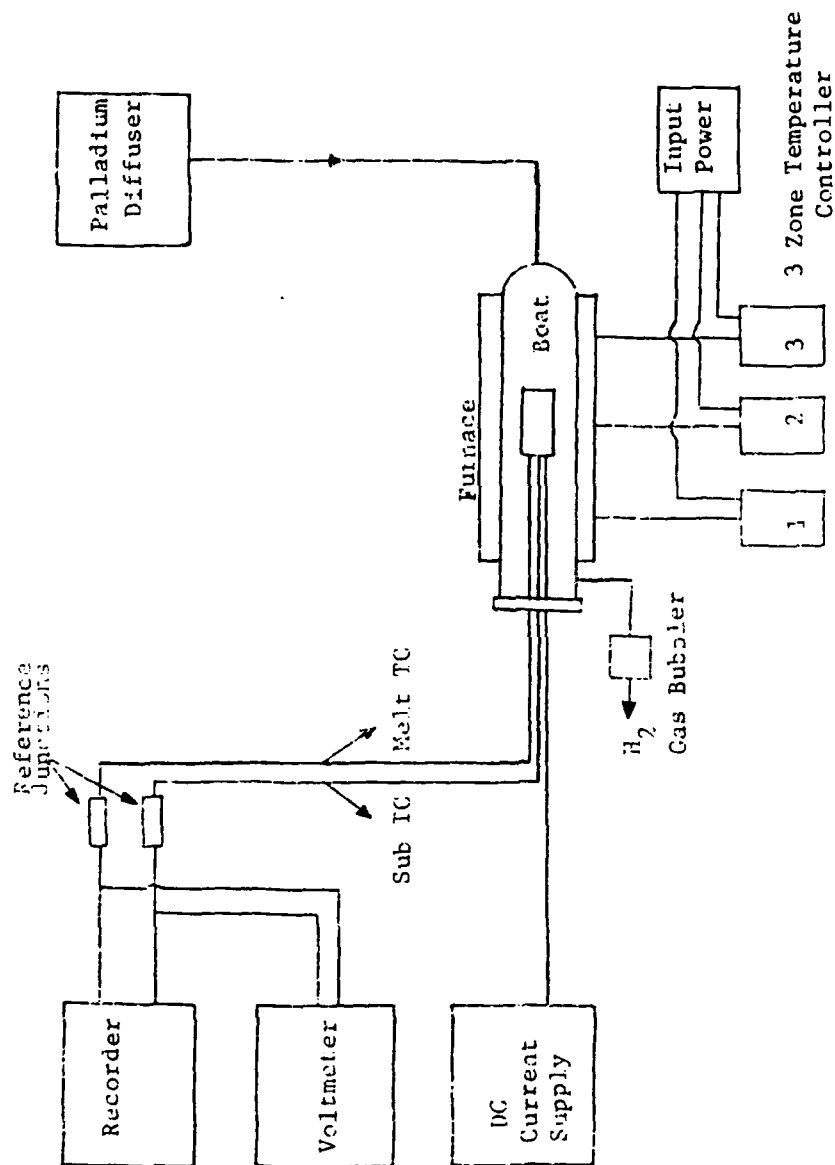
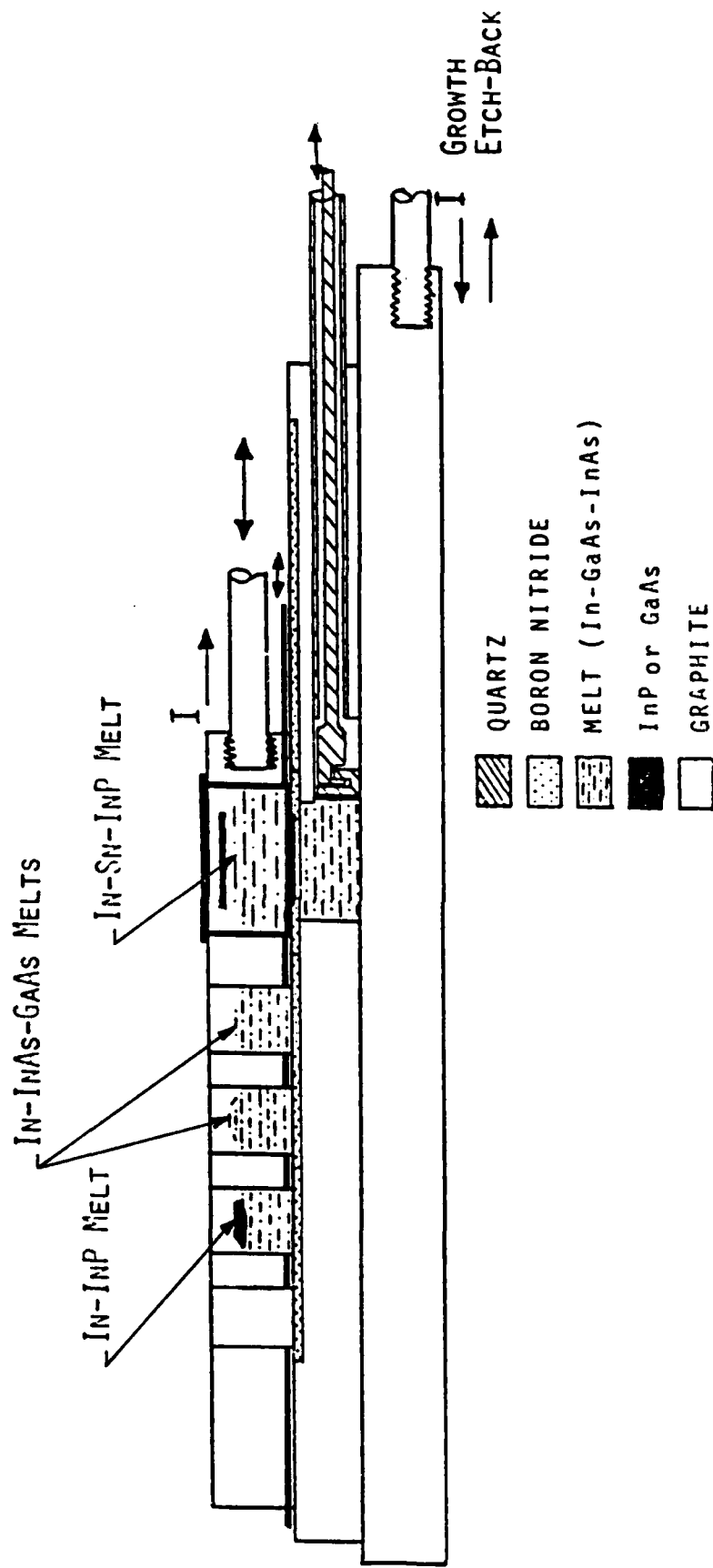Figure 1. A block diagram of the mdified liquid phase epitaxial growth system.

4

Figure 2. A schematic cross-section of the boat assembly used for electroepitaxial growth/etching of InP and GaAs

Prior to the commencement of the growth cycle, all the constituents of the growth melt were baked simultaneously for 48 hours at 670 °C in a hydrogen ambient. Excess amount of InP was used to replenish P evaporated during the extended melt saturation. This baking procedure was found to yield films of low carrier concentration. Thereafter a <100>-oriented InP substrate was loaded into the system and the solution was saturated for a period of 19 hours at 645 °C. Two solidus compositions were grown: $In_{.60}Ga_{.40}As_{.85}P_{.15}$ ($In_{.60}$, $\lambda=1.52$ μm) and $In_{.73}Ga_{.27}As_{.60}P_{.40}$ ($In_{.73}$, $\lambda=1.31$ μm). Growths were performed at a constant furnace temperature of 647 °C with a direct current density of 3 to 15 A/cm².

The thermal degradation of the substrate during such prolonged heating period was prevented by sliding the substrate underneath the graphite basket containing In-Sn-P solution. The enhanced solubility of P in the presence of Sn creates an overpressure of P, thereby minimizing the evaporation of high vapor pressure P from the InP substrate.

The growth rate was found to be a function of the composition of the quaternary layers. The growth rate of the $In_{.60}$ layers was almost six times larger than that of the $In_{.73}$ layers. Furthermore, layers thicker than 3μm could not be grown for $In_{.73}$ layers. The low growth rate of this material has been attributed to the fact that this composition lie in the micibility gap region. A similar trend of decrease in growth velocity with increasing P content in the solid was also observed in conventional thermal LPE as shown in Fig. 3.

Analytical values of the growth velocity for different compositions were calculated using Brysklewicz[10] model. It was assumed electromigration/electrotransport is the dominant mechanism contributing to the growth process. Differential mobility and diffusion coefficient of Ga were used as the fitting parameters and a good fit to the experimental data was obtained. It was found that diffusion coefficient of P and differential mobility of P were the rate

6

limiting factors for LPEE grown layers as in the case of thermal LPE.

In order to avoid the micibility gap in the phase diagram, growths of the
1.31 μm alloy were performed at 685 °C. Various melt baking sequences were
tried in order to reduce the residual carrier concentration. A low concentration
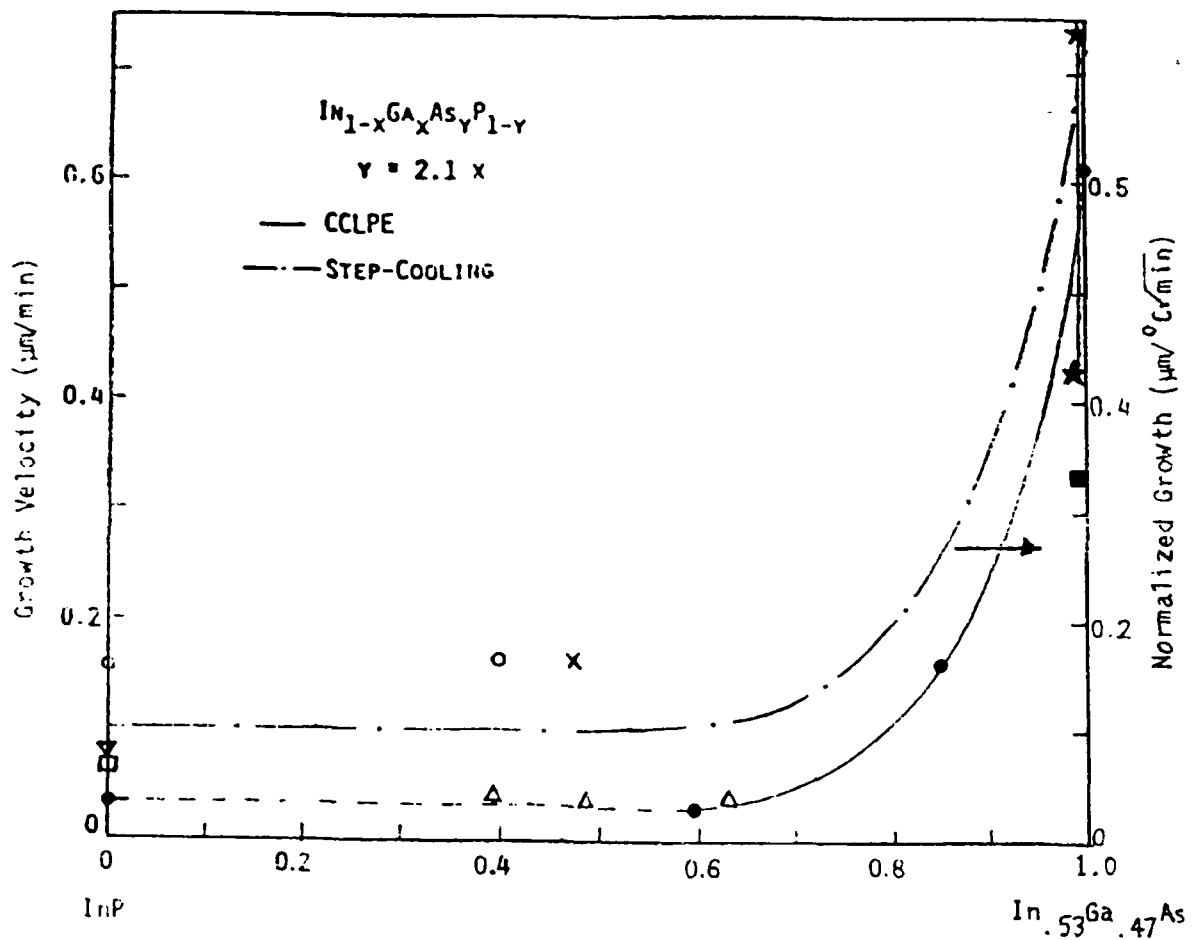of 1×10^{16} /cm^3 has been achieved.

Figure 3. Normalized growth rate vs. alloy composition. Growth
velocities from literature data are also shown.

Step-cooling: o Cook, et al.[11], x Kunishige, et al.[12],
△ Feng, et al.[13], □ Ishibashi, et al.[14],
∇ Hsieh, et al.[9]

Equilibrium
cooling: ★ Amano, et al.[15], ■ Pearsall, et al.[16]

7

2.3 CHARACTERIZATION OF Mn DOPED LAYERS

One of the other objective of the research project was to investigate suitable p-type dopant for device applications. Manganese (Mn) was chosen as it has been found[12,13] to be the best acceptor suitde for practical applications, for quaternary compositions closer to the ternary $In_{.53}Ga_{.47}As$. P-type InGaAsP layers with doping levels varying from $8x10^{16}$ /cm³ to $4x10^{18}$ /cm³ with excellent surface morphology were grown by liquid phase electroepitaxial technique.

The layers were characterized using X-ray diffraction, Hall and photoluminescence techniques at low temperatures ($77°K$). Analysis of temperature dependence of concentration data allowed the determination of the activation energy of the Mn-dopant level, donor and acceptor densities in the layer. The activation energy of the Mn acceptor level decreased from 57 meV to 32 meV with increasing hole concentration from $1x10^{17}$ /cm³ to $1.2x10^{18}$ /cm³. Temperature dependence of mobility data was analysed in terms of different scattering mechanisms prevalent in the layer, which also provided information on the acceptor and donor densities. In undoped layers, ionized impurity scattering is dominant for temperatures lower than $120°K$ while polar optical phonon and alloy scatterings account for the variation in mobility at higher temperatures. In doped layers, a good fit to the experimental data is obtained only when non-polar optical phonon and acoustic lattice mechanisms were taken into account as shown in Fig. 4. Both the Hall mobility and Hall constant data indicated a lower donor to acceptor concentration ratio than normally observed in p-type layers using the other dopants, indicating that Mn is an efficient dopant for InGaAsP layers.

Van Roosbroeck-Shockley model describes fairly well the spectral line shape of the quaternary layer if the absorption coefficient is assumed to vary exponentially with energy below the band gap. The qualitative features of the Mn level were deduced from the temperature and incident excitation level depe-

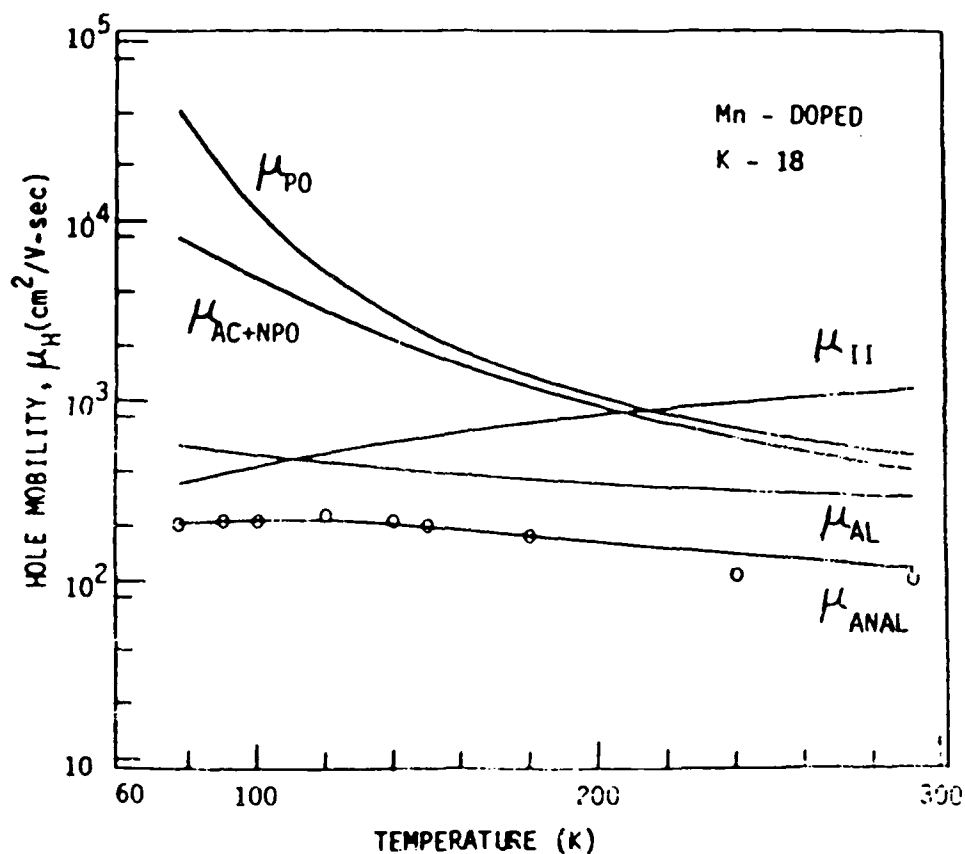ndence studies of PL emission peaks in doped layers.

Figure 4. Temperature variation of the hole mobility for Mn-doped
quaternary layer.

Detailed characterization of undoped and Mn-doped InGaAsP grown by
electroepitaxy is presented in Appendix B ("Properties of undoped
and Mn-doped InGaAsP grown by LPEE[17]" and "Characterization of Mn-doped
$In_{1-x}Ga_xAs_yP_{1-y}$ grown by LPEE[18]").

9

SELECTIVE ETCH-BACK AND GROWTH OF InGaAs

The interest in selective area etch-back of the substrate , prior to growth, lies with the inherent capability of establishing isolated channels and/or trenchs which can be refilled with another lattice-matched semiconductor compound. These isolated semiconductor regions can then be used as optical waveguides (long, narrow channels), or for device mesa structures (trenches).

To study the etch-back properties in (100)-oriented Fe-doped InP substrates, the substrates were pattern masked with ion beam sputtered quartz (SiO_2). The InP islands defined by the SiO_2 mask were of various sizes (80x1000 μm to 3000x3000 μm) and different geometries (narrow and wide strips, square, circular). The etch-back was performed at a constant furnace temperature of 640 °C by passing a direct electric current from the melt to the substrate for etch-back and from the substrate to the melt for growth. Current densities used were from 5 to 15 A/cm² for periods from 15 to 60 minutes.

Electroepitaxial etching profiles are examined by cleaving the (100) InP substrate in orthogonal directions along the (011') and (01'1') planes. Figure 5 is a SEM photomicrograph of an etched channel which shows the masking oxide (SiO_2), the sharp definition of the side walls, and the flat bottom (100) plane. The side walls are identified as (1'11)B and (1'1'1)A planes.

Our results show that etch-back by electroepitaxy is preferential. Narrow channels < 200μm wide and small trenches < 200x200 μm oriented parallel or perpendicular to the [011'] direction etched uniformly in the [100] direction revealing the (100) plane. At the same time, side etching proceeded

1c

up to the (111)A and (111)B planes, i.e., the (1'1'1)A, (1'11')A, (1'11)B, and (1'1'1')B
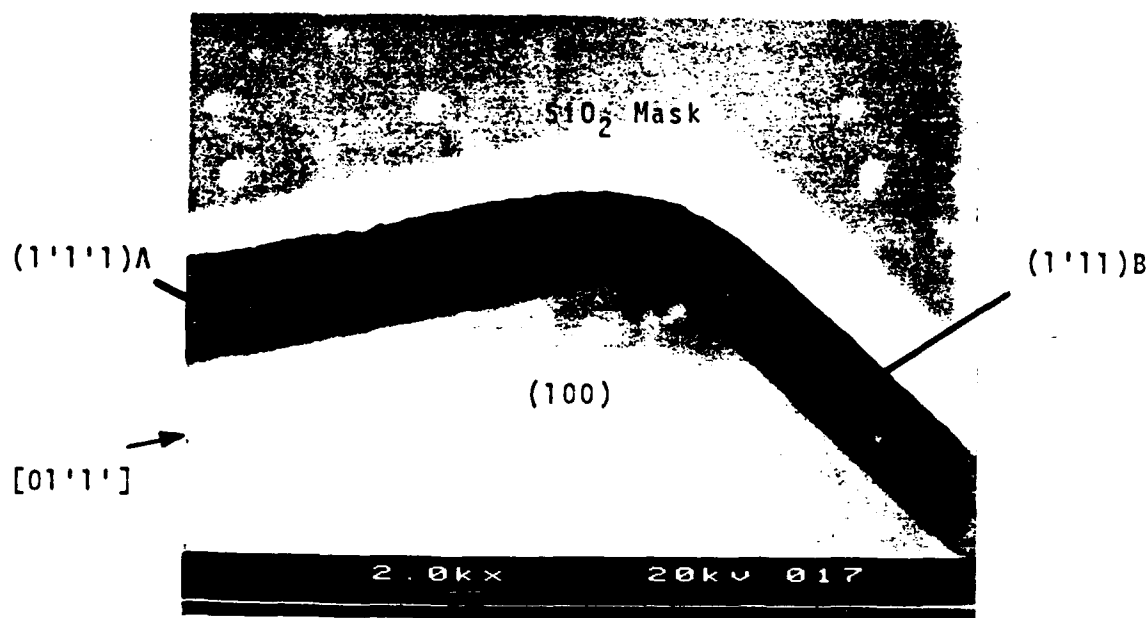

Figure 5. SEM photomicrograph of etched channel
on (100) InP substrate.

planes. Consequently, a trapezoid-shaped profile is obtained whose sides

form an angle of $54°58'$ with respect to the (100) surface. The side etch

proceeded fastest in the [011] directions. The order of magnitude of the etch

rate was (100) > (011) > (111)B > (111)A, while in chemical etching (in 1% Br_2-

Methanol) the order of magnitude of the etch rate was (011) > (111)B > (100)

> (111)A, and the etch rate on the (111)A planes was very slow. A more detai-

led analysis of selective etch-back and growth of InGaAs[19] was presented

during the 1987 Electronic Material Conference (EMC) in Santa Barbara, Califo-

rnia, June 23-27, 1987. A detailed paper about the subject will be submitted

to the Journal of Elect. Mater. Another paper (presented in Appendix B) about

selective electroepitaxial growth of $In_{0.53}Ga_{0.47}As$ on (100)-Fe:InP[20] was prese-

nted during the 1987 SOUTHEASTCON in Tampa, Florida, April 5-8, 1987.

11

SELECTIVE ETCH-BACK OF GaAs

Electroepitaxial etching was performed on (100), (111)A, and (111)B n-type (Si-doped) GaAs substrates[21]. Etch-back was performed at a constant furnace temperature of 800 °C by passing a direct electric current from the melt to the substrate. Current densities used in most of the experiments ranged from 5 to 17 A/cm^2. In few experiments , current densities ranging from 50 to 394 A/cm^2 were used. The etched samples were characterized by their surface morphology, etch depth, and etch pattern formed.

4.1   ETCH-BACK OF (100) GaAs

Figure 6a is a photomicrograph of an etch-revealed trench using SiO_2 masked substrate. The mask is a 7x7 array of 100x100 μm squares. The photomicrograph shows the mask opening, the sharp definition of the side walls, and the flat bottom of the (100) plane. The edges of the photomicrograph are parallel to the (011) cleavage planes. The etch-revealed facets demonstrate the anisotropic nature of GaAs. The trenchs are rotated 45° with respect to the square opening of the mask. Lateral etching varied according to crystallographic directions. The amount of the mask that extends over the etched trench was 20 μm in the [011] and [01'1'] directions, 9.5 μm in the [01'1] and [011'] directions, and 4.8 μm in the <110> directions. The undercutting rate of the (011) cleavage plane is very much faster than that of the (011') cleavage plane for the (100) substrate. This is because the exposed surfaces in the [011] direction are arsenic (As) surfaces. This faster etching in [011] direction is believed to account for the 45° rotation of etched trench with respect to mask opening.

12

The etch was performed at a current density of 10 A/cm2 for 35 minutes. The average depth of the etched trenchs is about 18 μm. The diamond-shaped trenches revealed no uneveness along the bottom Figure 6b is a photo-micrograph of a cleaved section. The figure shows the side walls slope down-ward towards each other forming a trapezoid-shaped profile. The measured angles formed by these side walls and the (100) surface were 54° 58'.

100 μ m

[100]
[011]
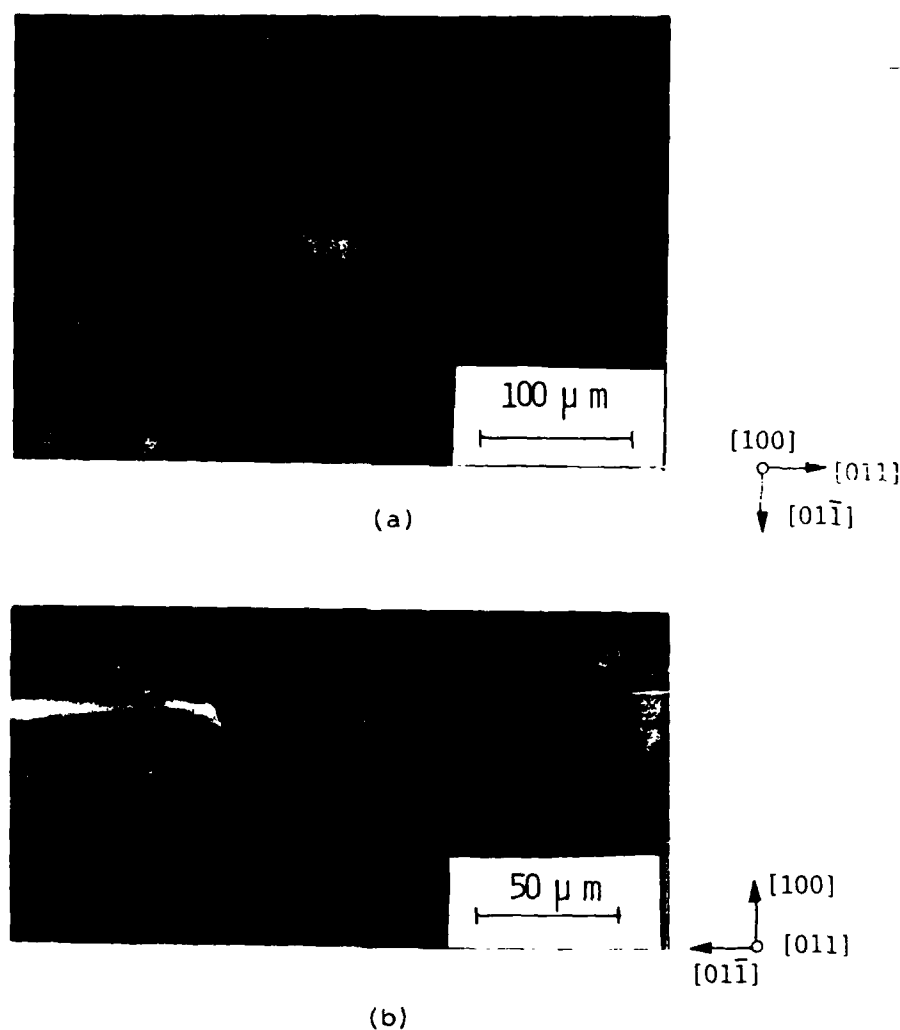[01$\bar{1}$]

(a)

50 μ m

[100]
[011]
[01$\bar{1}$]

(b)

Figure 6 (a) An trench revealed trench on the (100)oriented substrate;
(b) side view of a cleaved section. Etching was performed
at a current density of 10 A/cm2 for 35 minutes.

4.2 ETCH-BACK OF (111)A GaAs

Very little etching was observed in the windows on most of the etched
(111)A samples. Only small number of the windows (2-5 out of 49 windows)
revealed hexagonal shaped pattern when high current densities ranging from
50 to 394 A/cm2 were used.

Figure 7 is a photomicrograph of one of the etched trenches. Etching was
performed at a current density of 100 A/cm2 for 30 minutes. The average
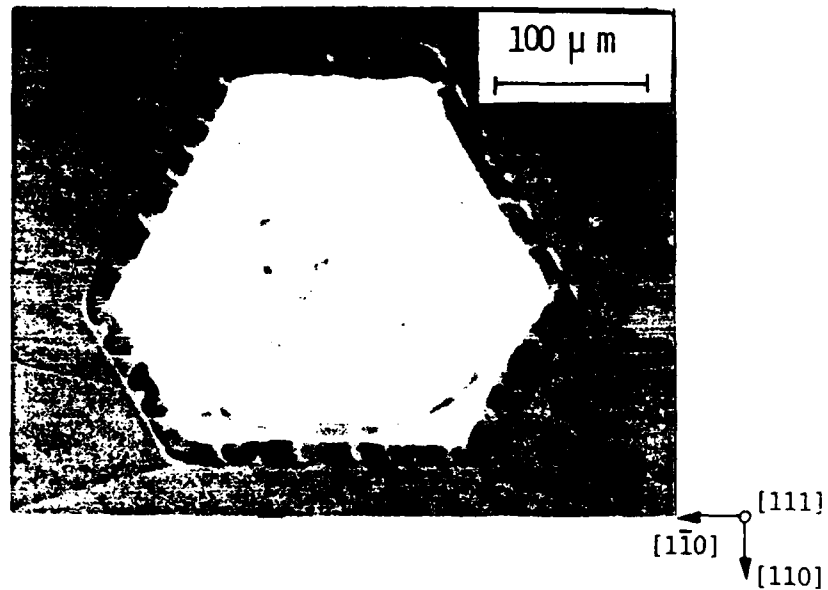etch depth is about 16 μm.

Figure 7. Etch revealed hexagonal trench on (111)A GaAs.
Etching was performed at a current density of
100 A/cm2 for 30 minutes.

Figure 7 shows the SiO_2 mask, the hexagonal trench and the tremendous
amount of lateral etching. The amount of lateral etching is about 96 μm in
the <111> directions and about 75 μm in the <011> directions. The side walls
of the hexagonal trench were identified as (111)A and (011), i.e., (1'11')A,
(1'1'1)A, (11'1')A, (01'1'), (101), and (110) planes.

14

4.3 ETCH-BACK OF (111)B GaAs

Figure 8 is a photomicrograph of an etch-revealed trench on (111)B GaAs. The electroepitaxial etch-back was performed at a current density of 5 A/cm² for 30 minutes.

The average etch depth of the (111)B trenchs was about 27 µm. Etch figures formed well defined equilateral triangles. Each side of the triangular pattern is parallel to a <011> direction.
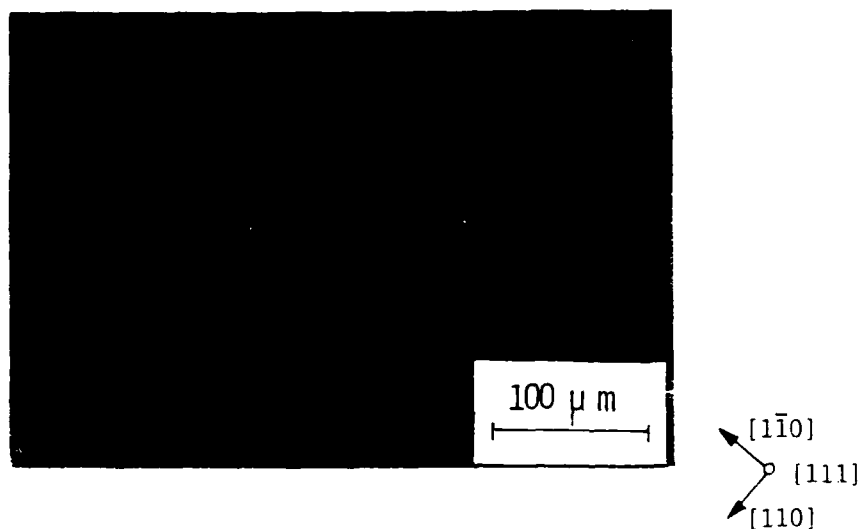

Figure 8. Electroepitaxial etch-revealed trench on (111)B GaAs. Etching was performed at a current density of 5 A/cm² for 30 minutes.

Figure 9a and b show the top and side view of a cross-sectioned trench. The cleaved section is slightly off center, along the (11̄0) cleavage plane. The measured angles formed by the right hand facet and the upper left hand facet (true angles) with respect to the (111)B surface are about 35° and 55°, respectively. Based on these measured angles, the etch-revealed side walls are identified as (110) and (111)B planes.

15

(a)

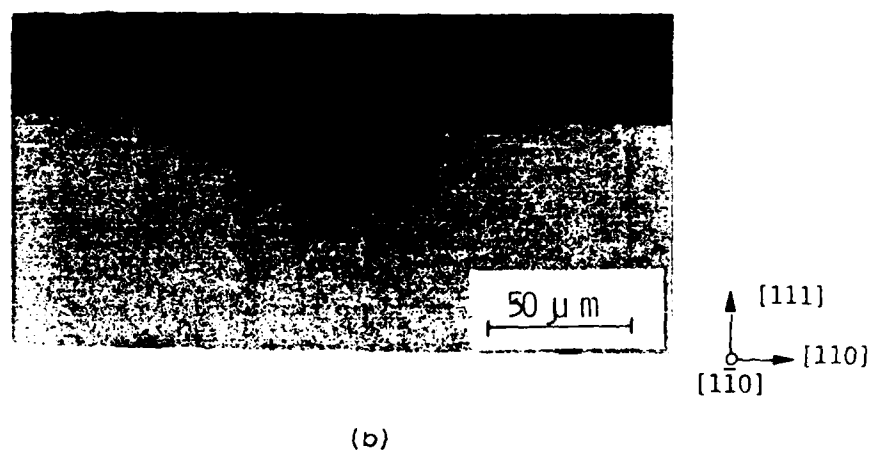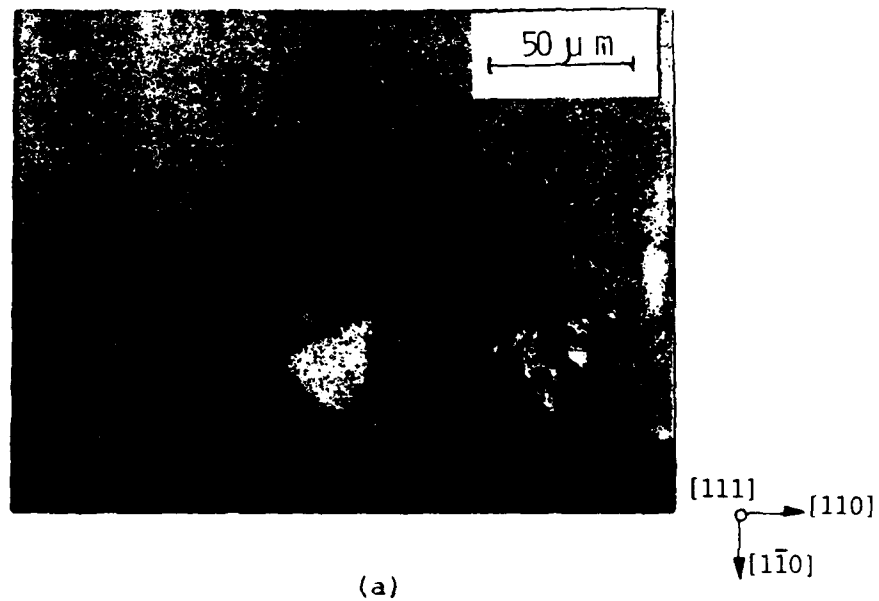[111] [110]
[1$\bar{1}$0]

(b)

[111]
[110]
[1$\bar{1}$0]

Figure 9   Cross-sectioned trench on (111)B GaAs: (a) top view;
(b) side view. Etching performed at a current density
of 5 A/cm2 for 30 minutes.

16

CONCLUSION AND RECOMENDATIONS

Significant progress was made in the growth of epitaxial InGaAsP and InGaAs lattice matched to (100) InP substrates by electroepitaxy, and in identifying some of the problems and effects which contributed to the high level of carrier concetration in the layers.

Electroepitaxy is a viable technique of growth of III-V ternaries and quaternaries and for etch-back of the substrate. It provides a means to grow/ etch-back at a constant furnace temperature, by passing direct electric current across the semiconductor melt interface for growth and across the melt semiconductor for etch-back. This is an advantage over other LPE techniques where the growth (etch-back) is not necessarily the alloy liquidus temperature.

The results of selective area etch-back by electroepitaxy showed that high quality etched surfaces without any undesirable roughness or etch pits can be obtained. The present results also indicate that selective etch-back using electroepitaxy may be useful in the fabrication of IC structures, since uniform trenches and/or channels with well defined shapes were obtained on both the (100) oriented and (111)B oriented substrates.

Further improvement in the quality and purity of materials grown by electroepitaxy can be achieved by minimizing the sources of impurities and possibly by remote loading the substrate.

17

V. REFERENCES

1. M. Kumagawa, A. F. Witt, M. Lichtensteiger, and H. S. Gatos, J. Electrochem. Soc., 120 , (1973).

2. D. J. Lawrence and L. F. Eastman, J. Elect. Mater., 6 , 1 (1976).

3. L. Jabstrzebski, H. C. Gatos and A. F. Witt, J. Electrochem Soc., 123, 1121 (1976).

4. L. Jabstrzebski, Y. Imamura, and H. C. Gatos, J. Electrochem. Soc., 125, 1140 (1978).

5. A. Abul-Fadl, and E. K. Stefanakos, J. Cryst. Growth, 39, 341 (1977).

6. J. J. Daniele, D. A. Commack, and P. M. Asbeck, J. Appl. Phys., 48, 914 (1977).

7. A. Abul-Fadl, E. K. Stefanakos, and W. J. Collis, J. Elect. Mater., 11, 559 (1982).

8 S. Iyer, E. K. Stefanakos, A. Abul-Fadl, and W. J. Collis, J. Cryst. Growth, 67, 337 (1984).

9. J. J. Hsieh, IEEE J. Quantum Elect. QE-17, 118 (1981).

10. T. Bryskiewicz, J. Lagowski, and H. C. Gatos, J. Appl. Phys., 51 ,988 (1980).

11. L. W. Cook, M. M. Tashima, and G. E. Stillman, Appl. Phys. Lett., 36 , 904 (1980).

12. O. Kunishige and S. Koichi, Appl. Phys. Lett., 33 , 449 (1978).

13. M. Feng, T. H. Windhorn, M. M. Tashima, G. E. Stillman, Appl. Phys. Lett., 32, 758 (1978).

14. T. Ishibashi, Y. Imai, and M. Ida, J. Electrochem. Soc., 128 , 1776 (1981).

15. T. Amano, T. Nagai, Jap. J. Appl. Phys., 20 , 2105 (1981).

16. T. P. Pearsall, R. Bisaro, R. Ansel, and P. Merenda, Appl. Phys. Lett., 32 , 497 (1978)

17. S. Iyer, A. Abul-Fadl, W. J. Collis, and M. Khorrami, Thin Solid Films, 163, (1988).

18. S. Iyer, A. Abul-Fadl, W. J. Collis, and M. Khorrami, Epitaxy of Semiconductor Layered Structures, Proc. of the Mater. Res. Soc., 102, 201 (1988).

19. A. Abul-Fadl, W. J. Collis, S. Maanaki, T. McCarty, and S. Iyer, Presented during the 1987 Elect. Mater. Conf., Santa Barbara, Calif., June 5-8, (1987).

20. A. Abul-Fadl, S. Maanaki, W. J. Collis, and S. Iyer, Presented during the 1987 SOUTHEASTCON. Tampa, Florida. April 5-8, (1987).

21. T. McCarty, Master thesis (EE), August 19, 1988.

APPENDIX A

Theses

"Selective Electroepitzaxial Growth of $In_{0.53}Ga_{0.47}As$ on (100) Fe-doped InP", by Samir Maanaki

"Selective Etch-back of (100), (111)A, and (111)B GaAs by Electroepitaxy", by Taunya A. McCarty

"Characterization of Undoped and Mn-doped InGaAsP Grown by LPEE", by Mohammad N. Khorrami

ABSTRACT

SELECTIVE ELECTROEPITAXIAL GROWTH OF In$_{0.53}$Ga$_{0.47}$As

ON (100) Fe-doped Inp

by Samir M. Maanaki

(Dr. Ali Abul-fadl, Advisor)

Electroepitaxy has been used to grow InGaAs on selected (100) InP islands using a sputtered SiO$_2$ layer as the substrate mask. The growth was performed by passing low direct electric current of 1A for 15 minutes across the substrate-melt interface with a constant furnace temperature of 640 °C. The epitaxial layers were characterized with respect to their surface morphology and thickness uniformity. It was found from the experimental results that a uniform layer with excellent surface morphology can be achieved on small regions as wide as 200μm and on circles with diameter of less than 500μm. Also it was found that the electric field intensity along the substrate-melt interface of the islands is dependent upon the geometry of the growth regions. Poisson's equation was solved by the finite element method to show the relation between the intensity of the field and the uniformity of growth in various regions.

21

SELECTIVE ETCH-BACK OF (100), (111)A, and (111)B GaAs by ELECTROEPITAXY

By Taunya A. McCarty

(Dr. Ali Abul-Fadl, Adviser)

Selective etch-back of silicon dioxide masked (100), (111)A, and (111)B (Si-doped) GaAs substrates was performed by electroepitaxy. The etch-back of the substrates was done at a constant furnace temperature of $800^{\circ}C$ by passing a direct electric current from the melt to the substrate. The current densities used were in the ranges of 5 to 17 A/cm^2 and 50 to 394 A/cm^2. The time periods ranged from 10 to 60 minutes. A 7 X 7 array pattern was used as the mask. The mask openings were either 100 X 100 μm squares, 500 X 500 μm squares or 234 μm diameter circles. The etch-back results will be presented. Geometric models which were used as an aid in determining crystallographic information shall be introduced. A comparison was made between the experimental and theoretical results and the results obtained by other researchers using wet chemical etching. Electroepitaxial etching delivered satisfactory results. Thus, this etching process can become very useful in the fabrication of integrated circuit devices. It has the possibility of being used to make isolated channels and/or trenches in which another lattice-matched semiconductor compound can be grown. These isolated semiconductor regions can then be used as optical waveguides or device mesa-structures (i.e., laser diode arrays) [18,47].

22

CHARACTERIZATION CF UNDCPED AND Mn-DOPED
InGaAsP GROWN BY LPEE

by Mohammad N. Khorrmi

(Dr. S. Iyer, Advisor)

IN PREPARATION

APPENDIX B

Papers

"Properties of Undoped and Mn-doped InGaAsP by LPEE", Thin Solid Films, 163 ,(1988).

"Characterization of Mn-doped $In_{1-x}Ga_xAs_yP_{1-y}$ Grown by LPEE", Epitaxy of Semiconductor Layered Structures, Proc. of the Mater. Res. Soc., 102 , (1988).

"Selective Electroepitaxial Growth of $In_{0.53}Ga_{0.47}As$ on (100)-Fe:InP", Proc. of the 1987 SOUTHEASTCON, 1 , (1987).

PROPERTIES OF UNDOPED AND Mn-DOPED InGaAsP GROWN BY LPEE

SHANTHI N. IYER, ALI ABUL-FADL, WARD J. COLLIS AND
MOHAMMAD N. KHORRAMI

North Carolina A&T State University, Greensboro, NC, USA

ABSTRACT

Undoped and Mn-doped InGaAsP epilayers lattice matched to InP substrate have been grown by the liquid phase electroepitaxial (LPEE) technique. The dependence of growth velocity on current density of both undoped and doped layers has been studied. Layers of good surface morphology with hole concentrations in the range of $8 \times 10^{16}/cm^3$ to $4 \times 10^{18}/cm^3$ have been achieved. Activation energy of the Mn-acceptor level was estimated to vary from 57 to 32 meV with increasing hole concentration. Temperature dependence of carrier mobility data was analysed in terms of different scattering mechanisms and the values of acceptor and donor densities determined were compared with those obtained from temperature variation of Hall concentration data. Dependences of photoluminescence peak energy and intensity on the temperature and incident excitation levels have been investigated.

INTRODUCTION

Liquid phase epitaxy has been one of the extensively used and preferred growth technique for InGaAsP compounds. Liquid phase electroepitaxial technique (LPEE) differs from the conventional liquid phase epitaxial technique in that the growth is primarily controlled by the current density passing through the melt-substrate interface at the liquidus temperature. As the growth is carried out at a constant furnace temperature, this technique facilitates better control on the thickness[1] and doping of the layer[2]. Further, it has been shown that layers grown by this technique exhibit better compositional homogeneity[3,4] with improved interface stability[5] and surface morphology[6].

In our previous paper[7], we have reported the growth of InGaAsP layer lattice matched to InP by LPEE technique in the entire composition range of the quaternary alloy. However, thick layers of good quality (surface morphology) were difficult to grow for compositions in the middle of the alloy range, which was attributed to the presence of the miscibility gap. This problem has been circumvented by raising the growth temperature to 685^0 C as suggested by Schemmel et al.[8], where a stable composition can be grown.

In this paper, we report the growth of nominally pure and Mn- doped quaternary layers corresponding to a photoluminescence peak wavelength of 1.34 μm. The temperature dependence of carrier concentration and mobility were investigated in detail, to estimate the activation energy of the Mn dopant and the dominant scattering mechanisms limiting the mobility of carriers, respectively. In addition, luminescence of the undoped and Mn-doped layers was also studied.

EXPERIMENTAL

The growth method utilizes the conventional horizontal slider boat system modified to permit the passage of electric current through the substrate-melt interface. The details of the growth system and the substrate preparations have been described elsewhere[7,9]. Semi-insulating (100) oriented InP wafers of 0.4 mm (16 mil) thickness and 1x1 cm in area were used as the substrates. Elemental 4N purity Mn was used as the source material for Mn concentrations in the melt exceeding 10^{-3}. For lower concentrations Mn diluted with In, and baked at 740^0 C for homogenization, was used as the dopant source.

The baking of the source materials In, InAs, and GaAs was carried out at 740^0C for approximately 16 hours, and then the temperature was gradually lowered to 685°C in approximately 18 hours. An additional baking of 24 hours was carried out after the addition of Mn in the case of Mn-doped quaternary layers. InP substrate and undoped InP source, which was added in excess, are then loaded and saturated for approximately 8 hours, prior to initiation of the growth.

Hall effect measurements were carried out using van der Pauw method on clover leaf shaped samples in a magnetic field of 3 KG. The Hall scattering factor was assumed to be unity[10,11] in the temperature range (60K-300K) investigated. Photoluminescence measurements were carried out using the argon-ion laser as the excitation source with a 1/2-m monochromator and a lead sulfide detector with conventional lock- in techniques for dispersion and detection purposes, respectively.

RESULTS AND DISCUSSION

A. GROWTH VELOCITY AND SURFACE MORPHOLOGY

The growth velocity of the undoped and Mn-doped quaternary epilayers was studied as a function of current density ranging from 3 A/cm² to 12 A/cm². Though there is a considerable scatter in the data as illustrated in Fig. 1, the growth velocity appears to increase linearly with current density indicating electromigration to be the dominant mechanism contributing to the growth process. The growth velocity of the undoped quaternary is typically 6μm/hr at a current density of 10 A/cm² which is almost twice the growth velocity[7] achieved at 650°C but lower than Mn-doped layers.

Both the undoped and doped layers exhibit large positive lattice mismatch of ~0.2%. Lattice mismatch is found to be a function of the baking temperature and duration. A fine terracing is observed in undoped layers while the surface morphology of the doped layers is excellent (mirror smooth) up to a Mn concentration of 2×10^{-3}. At higher doping levels, the layers are rough and for concentrations exceeding 10^{-2} epilayers are of so poor quality that the growth melt cannot be wiped off from the top of the substrate.

B. ELECTRICAL PROPERTIES

The unintentional doped quaternary layer is normally n-type, and Mn-dopant renders it p-type. A Hall mobility of typically 4712 and 98 cm²/V-sec has been achieved in undoped and lightly doped layers, respectively. Undoped samples exhibit background carrier concentration of 1×10^{16}/cm³ which is found to be invariant with temperature in the range of 60K-300K indicating the occurance of impurity band conduction at these concentration levels. Figure 2 shows the variation of hole concentration with temperature in the range of 60K-300K for doped films. The data were analysed using the expression for carrier concentration in n-type

non-degenerate semiconductors, where the acceptor activation energy (E_A), donor (N_D), and acceptor (N_A) densities are treated as the fitting parameters. The values of these parameters that resulted in a best fit with the linear portion of the experimental data near room temperature, are listed in Table 1. The activation energy of the acceptor level decreases from 57 meV to 32 meV with increasing hole concentration indicating broadening of the impurity band. The computed value of donor to acceptor ratio is low ranging from 0.05 to 0.2.

The acceptor and donor concentrations were likewise estimated from the analysis of temperature variation of Hall mobility data, which also provides information on the scattering mechanisms prevalent in the layer. Contributions of different scattering mechanisms to the mobility were taken into account using Matthiessen's rule. In undoped layers, ionized impurity scattering is dominant for temperatures lower than 120K while polar optical phonon and alloy scatterings account for the variation in mobility at higher temperatures as shown in Fig.3. The equations used for the computation of individual scattering mechanisms are given in Ref. 12 and the parameters used in the calculation of carrier mobility are listed in Table 2. The value of electron effective mass is taken from Nicholas et al.[13], while the rest of the parameters have been estimated from the linear interpolation of the values from the binary constituents. Total impurity concentration, $N_D + N_A$, and the scattering potential, ΔU, were used as the adjustable parameters. A good fit to the experimental data (as shown in Fig.3) is obtained for $N_D + N_A = 3 \times 10^{16}/cm^3$, which yields a compensation ratio N_A/N_D of 0.5 normally observed in these layers[11,14,15]. The estimated value of scattering potential, 0.7, is in excellent agreement with the value reported by Hayes et al.[14] and Bhattacharya et al.[10] but higher than the value of 0.62 reported by Greene et al.[11]. In doped layers a good fit to the experimental data is obtained only when non-polar optical phonon and acoustic lattice

scattering mechanisms were taken into account (Fig.4). The parameters used for the computation of the mobility are also included in Table 2. A good fit to the experimental data has been obtained in all the doped samples for $\Delta U_P=0.2$ which is close to the value of 0.28 determined by Hayes et al.[14].

The values of N_D^- and N_A^- estimated from the mobility data are larger than the corresponding values estimated from the temperature dependence of the concentration data. The large discrepancy between these two values could be attributed to any one or combination of the following. (a) The absence of strong freeze out in these layers suggest the impurity banding, which makes the estimated values from both the analysis inaccurate, with the mobility data tending to overestimate the values of N_D^- and N_A^-. (b) The computation of the ionized impurity scattering using Brooks-Herring formula at these high doping levels could have significant effect in the calculated mobility values. In fact, a good fit could not be obtained for sample K-29 which has a room temperature carrier concentration of $1.2 \times 10^{18}/cm^3$. However, the analysis of both the mobility and Hall constant data indicate somewhat lower compensation in these layers than normally observed in p-layers using the other dopants [16,17].

C. PHOTOLUMINESCENCE

The general nature of the photoluminescence (PL) spectra of the undoped sample is as shown in Fig.5. The spectrum is asymmetric being broader at high energy side. Line shape analysis was carried out using generalized form of van Roosbroeck-Shockley's expression for the emission rate given by

$$I(\hbar\omega) \propto \alpha(\hbar\omega) \exp(-\hbar\omega/kT)/\lambda^2$$

where $\alpha(\hbar\omega)$ is the absorption coefficient near the band edge. It is taken as

$$\alpha(\hbar\omega) = A \exp[(\hbar\omega - E_G)/\sigma kT] \text{ for } \hbar\omega \leq E_G$$

30

$$= B \ (\hbar\omega - E_G)^{1/2} \ \text{for} \ \hbar\omega \geq E_G$$

where A, B, σ and E_G are the adjustable parameters. σ determines the shape of the PL response. Fairly good fit to the experimental PL response is obtained for σ =0.4 and E_G=0.915 eV. The value of σ=0.4 is close to the value of 0.3 determined by Temkin et al.[18].

Figure 6 depicts the observed variation in PL peak energy with temperature. Assuming that the shift in energy band gap is reflected in the shift in PL peak energy, the temperature dependence of peak position of the band edge emission is found to be very well described by Varshni's formulation[19]

$$E(T) = E(0) - \alpha T^2/(\beta + T)$$

where the values of α and β are as determined by Temkin et al.[18]. The PL intensity is found to decrease with temperature while the full width at half maxima increases with temperature as expected.

The Mn-doped layers are characterized by an additional broad band peak related to donor-acceptor (DA) transitions displaced towards the lower energy side by 38meV as shown in Fig.7. The relative intensity of these two peaks is dependent on the incident laser power. As the incident excitation level increases, band edge (BE) emission increases very rapidly relative to the intensity of the broad band peak, ultimately the BE peak becomes dominant. For layers with higher doping levels , BE emission peak becomes dominant at a much higher excitation levels. This phenomenon may be explained by the fact that at low excitation levels, excited free holes become bound to the ionized acceptors. As the intensity increases, most of the acceptors become neutralized resulting in saturation of the donor to acceptor transitions. Further increase in incident excitation level leads to number of free holes exceeding the number of acceptors and hence band to band transitions start

dominating. For layers of higher doping levels, as the number of holes required to neutralize the ionized acceptors are larger, higher excitation levels are necessary for the onset of saturation of DA transitions.

The variation of photoluminescence spectra of doped samples with temperature (Figure 8) indicates little variation in the position of the emission peak up to a temperature of 80 K. However, the intensity of DA emission decreases with temperature allowing the band to band transition to dominate at higher temperatures. The temperature at which this occurs depends on the incident excitation level. This is accounted by the presence of more free carriers in the valence and conduction bands and hence increasing the probability of band to band recombination with temperature. The variation of PL emission spectra with temperature and incident excitation level thus confirm the initial assignment of the two peaks. Mn signature is also observed in undoped layers but much weaker in intensity, indicating that Mn is one of the contaminants at low concentrations in InGaAsP layer.

CONCLUSION

Undoped and Mn-doped InGaAsP layers have been grown by LPEE technique. Lightly doped layers exhibit excellent surface morphology. The growth velocity of undoped layers is typically 6μm/hr at a current density of 10 A/cm^2 and is much lower than the growth velocity of doped layers. Maximum hole concentration of 4×10^{18}/cm^3 has been obtained in doped layers. The activation energy of the Mn acceptor level decreased from 57 meV to 32 meV with increasing hole concentration from 1×10^{17}/cm^3 to 1.2×10^{18}/cm^3. The values of the acceptor and donor densities determined from the Hall mobility data are consistently higher than the respective

32

values determined from the Hall constant data. The values of alloy scattering potential for undoped and Mn-doped layers were found to be 0.7 eV and 0.2 eV, respectively.

van Roosbroeck-Shockley model describes fairly well the spectral line shape of the undoped quaternary layer if the absorption coefficient is assumed to vary exponentially with energy below the band gap. The qualitative features of the Mn level were deduced from the temperature and incident excitation level dependence studies of PL emission peaks in doped layers.

ACKNOWLDGEMENTS

REFERENCES

1. L. Jastrzebski, Y. Imamura and H.C. Gatos, J. Electrochem. Soc. 125(1978)1140

2. J. Lagowski, L. Jastrzebski and H.C. Gatos, J. Appl. Phys. 51(1980)364.

3. J.J. Daniele and A.J. Hebling, J. Appl. Phys. 52(1981)4325.

4. J.J. Daniele and A. Lewis, J. Electron. Mater. 12(1983)1015.

5. A. Okamoto, J. Lagowski and H.C. Gatos, J. Appl. Phys. 53(1982)1706.

6. Y. Imamura, L. Jastrzebski and H.C. Gatos, J. Electrochem. Soc. 125(1978)1560.

7. S. Iyer, E.K. Stefanakos, A. Abul-Fadl and W.J. Collis, J. Cryst. Growth 70(1985)162.

8. G.Schemmel, R. Dorn, K. Hess, R. Linnebach, K. Losch, Proc. 10th Int. Symp. on GaAs and related compounds, Albuquerque, Inst. Phys. Conf. Ser. 65(1983)209.

9. A. Abul-Fadl, E.K. Stefanakos and W.J. Collis, J. Electron. Mater. 11(1982)559.

10. P.K. Bhattacharya, J.W. Ku, S.J.T. Owen, G.H. Olsen and S. Chiao, IEEE J. Quantum Electron. QE-17(1981)150.

11. P.D. Greene, S.A. Wheeler, A.R. Adams, A.N. El-Sabbahy and C.N. Ahmad, Appl. Phys. Lett. 35(1979)78.

12. J.R. Hayes, A.R. Adams and P.D. Greene, in InGaAsP Alloy Semiconductors edited by T.P. Pearsall (Wiley, New York, 1982), p.189.

13. R.J. Nicholas, J.C. Portal, C. Houlbert, P. Perrier and T.P. Pearsall, Appl. Phys. Lett. 34(1979)492.

14. J.R. Hayes, D. Patel, A.R. Adams and P.D. Greene, J. Electron. Mater.

11(1982)155.

15. J.L. Benchimol, D. Scalbert and M. Quillec, J. Electron. Mater. 14(1985)655.

16. Mulpuri V. Rao, J. Appl. Phys. 58(1985)4313.

17. T.P. Pearsall, G. Beuchet, J.P. Hirtz, M. Visentin, M. Bonnet and A. Roizes, Proc. of the 8th Int. Symp. on GaAs and Related Compounds, Inst. Phys. Conf. Ser. 56(1981)639.

18. H. Temkin, V.G. Keramidas, M.A. Pollack and W.R. Wagner, J. Appl. Phys. 52(1981)1574.

19. Y.P. Varshni, Physica 34(1967)149.

TABLE 1. Electrical properties of Mn-doped quaternary layer

Sample No.	p (cm^{-3}) at RT	μ (cm^2/V-sec)	E_A (meV)	N_A (cm^{-3})	N_D cm($^{-3}$)	$N_D{}^{\cdot}$ (cm^{-3})	$N_A{}^{\cdot}$ (cm-3)
K-18	1.6×10^{17}	97	57	3×10^{17}	4×10^{16}	7×10^{17}	4×10^{17}
K-22	4.1×10^{17}	85	45	4.5×10^{17}	3×10^{16}	9×10^{17}	4.5×10^{17}
K-25	6.3×10^{17}	84	32	8.5×10^{17}	4.5×10^{16}	2.2×10^{18}	1.2×10^{18}
K-29	1.2×10^{18}	65	32	3×10^{18}	5×10^{17}	-	-

TABLE 2. The values of physical parameters used in the computation of analytical electron and hole mobilities in undoped and Mn-doped layers.

Parameter	value
$e^{\cdot}/e$	0.23
$m_e{}^{\cdot}/m_o$	0.055
$m_l{}^{\cdot}/m_o$	0.064
$m_h{}^{\cdot}/m_o$	0.687
$\theta(K)$	426
$E_{AC}(eV)$	3.389
$E_{NPO}(eV)$	6.107
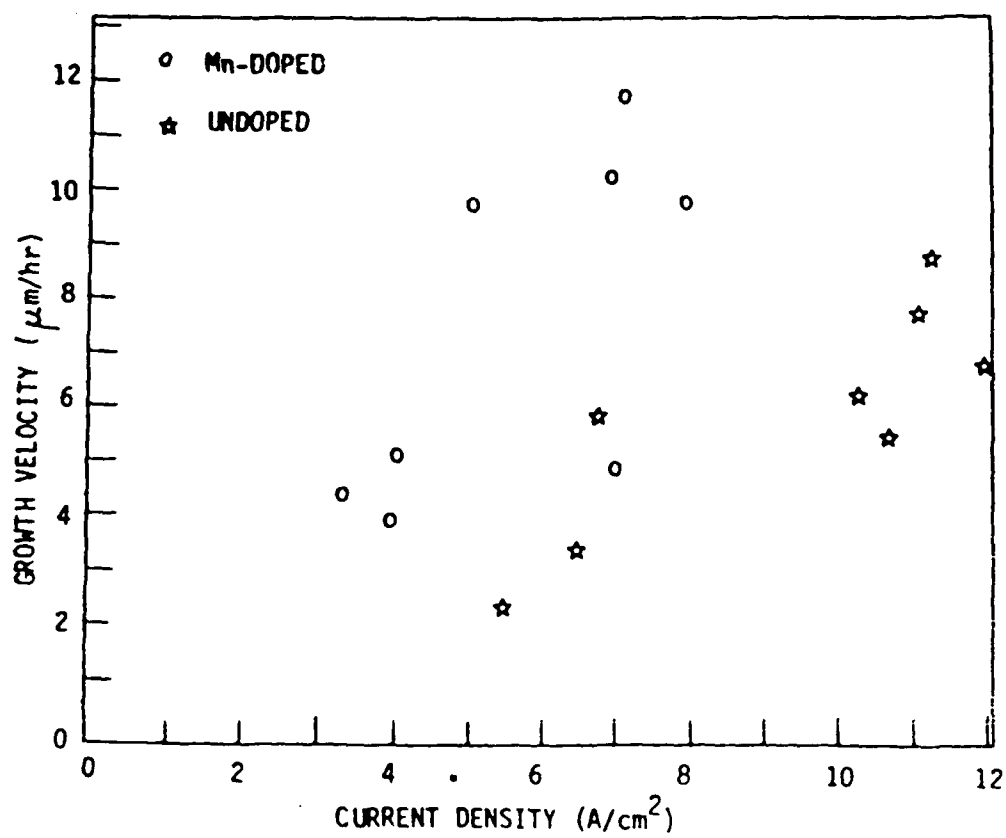
Figure 1. Growth velocity versus current density for LPEE grown undoped and Mn-doped InGaAsP layers.
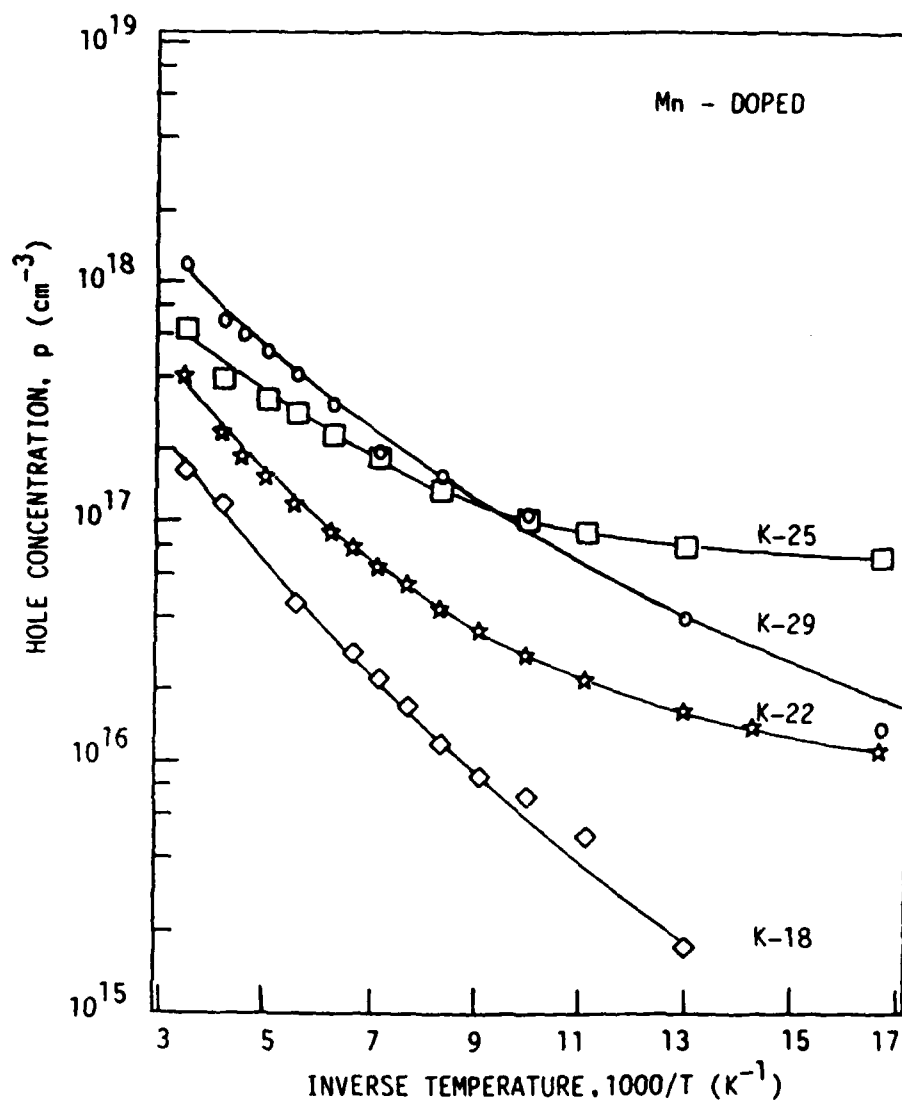
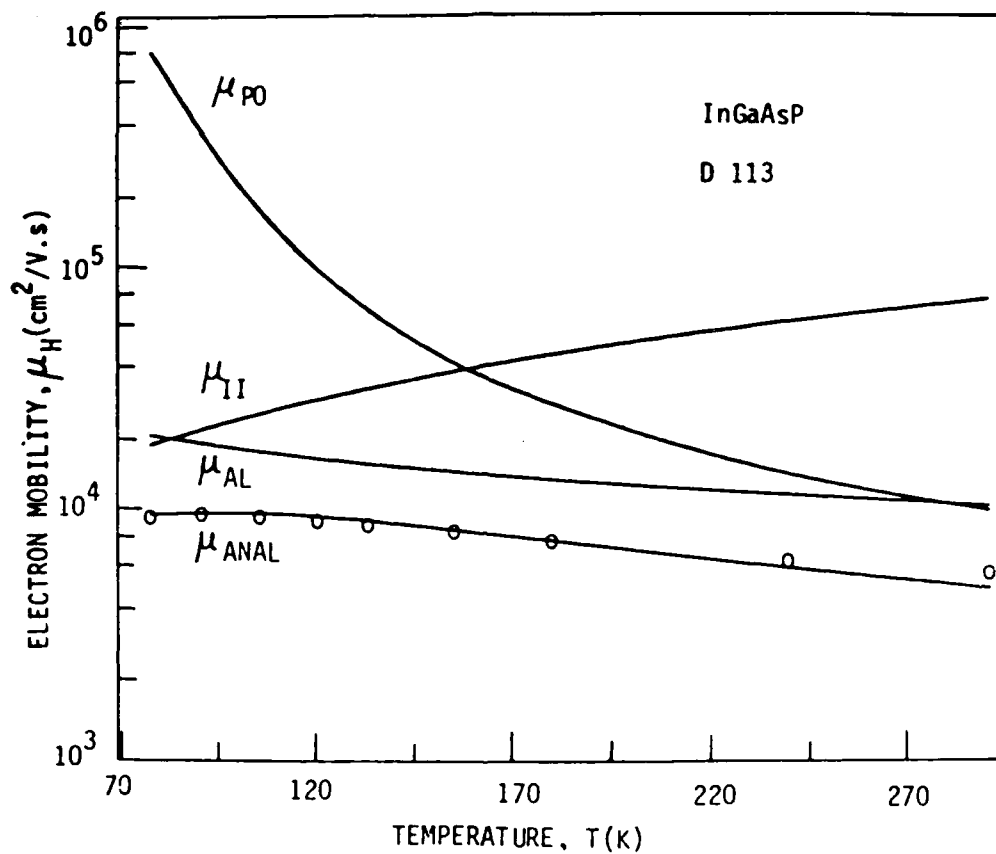Figure 2. Temperature dependence of hole concentration for Mn-doped layers.

Figure 3. Temperature dependence of Hall mobility for undoped
quaternary layer sample D 113. The solid line through
the data points is the computed value of the
mobility taking into account (a) μ_{II}, ionized impurity
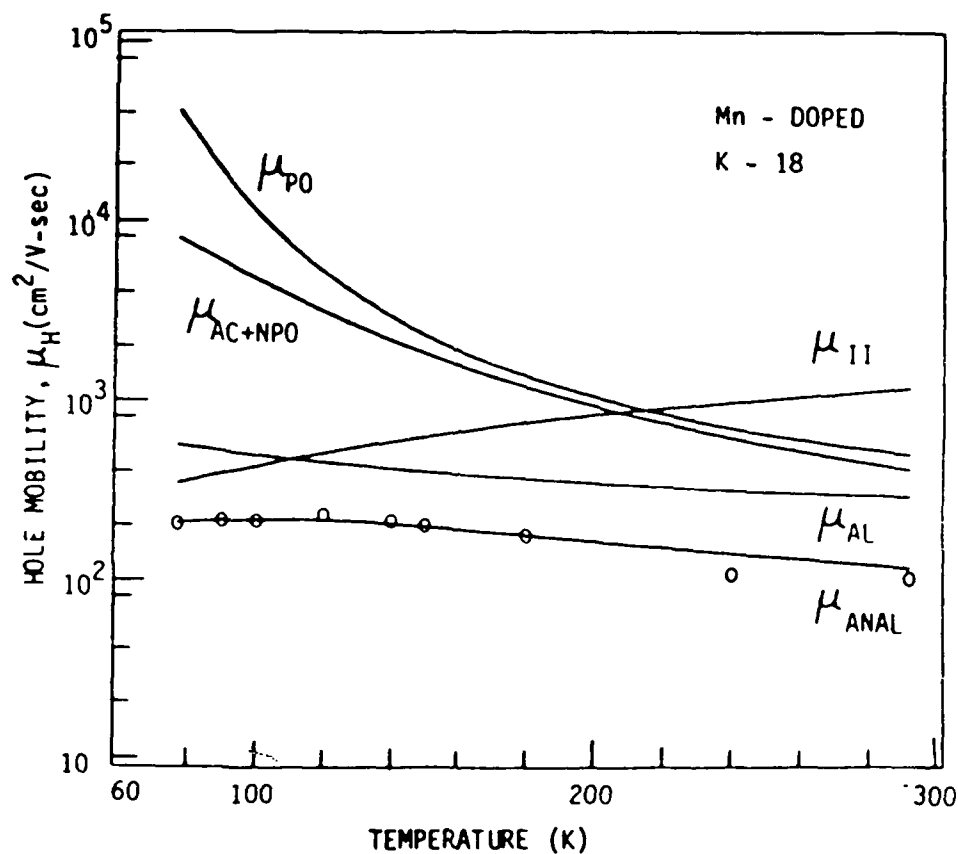scattering, (b) μ_{AL}, alloy scattring and (c) μ_{PO}, polar
optical phonon scattering.

Figure 4. Temperature variation of the hole mobility for Mn-doped quaternary layer(sample K-18). The solid line through the data points is the computed value of the mobility taking into account the different scattering mechanisms, namely, (a) μ_{II}, ionized impurity scattering, (b) μ_{PO}, polar optical phonon scattering, (c) μ_{AL} alloy scattering and (d) μ_{AC+NPC}, non-polar optical and acoustic scattering.
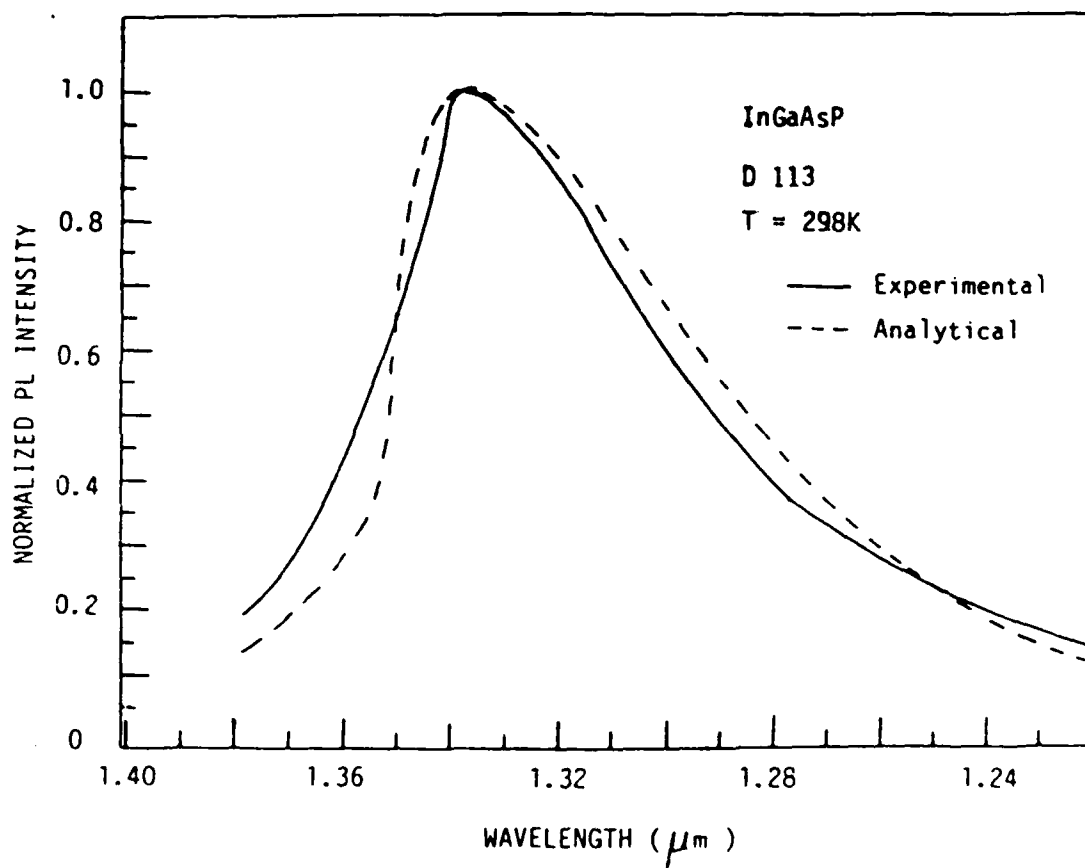
Figure 5. Comparison between the experimental and theoretically generated line shapes using the van Roosbroeck-Shockley model.

41
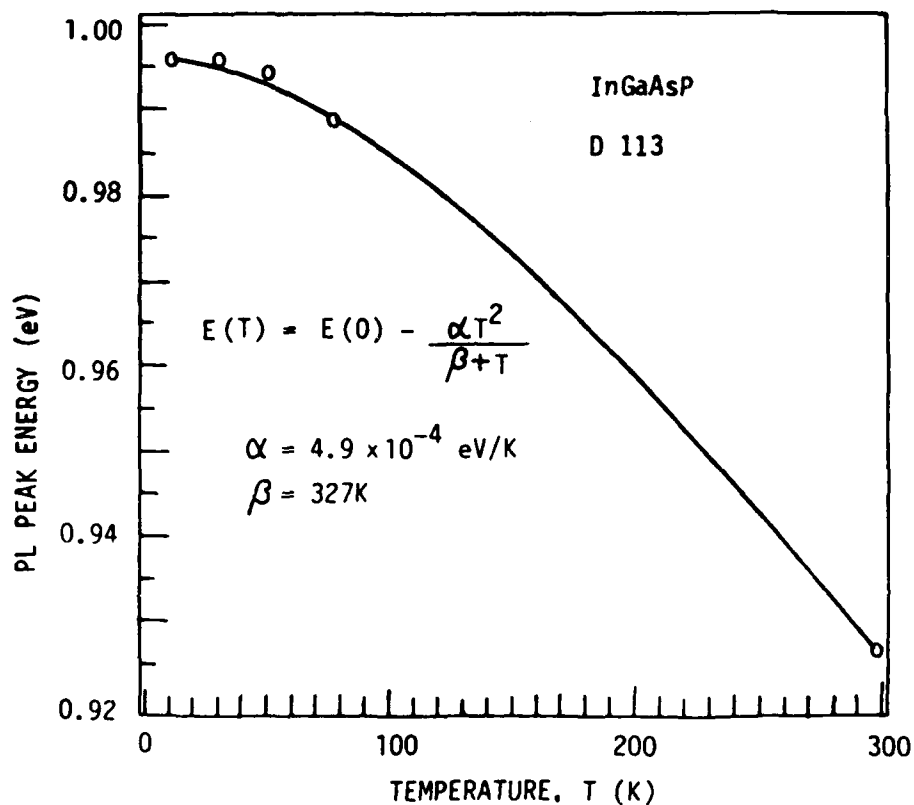
Figure 6. The solid line through the data points represent
the analytically determined temperature variation
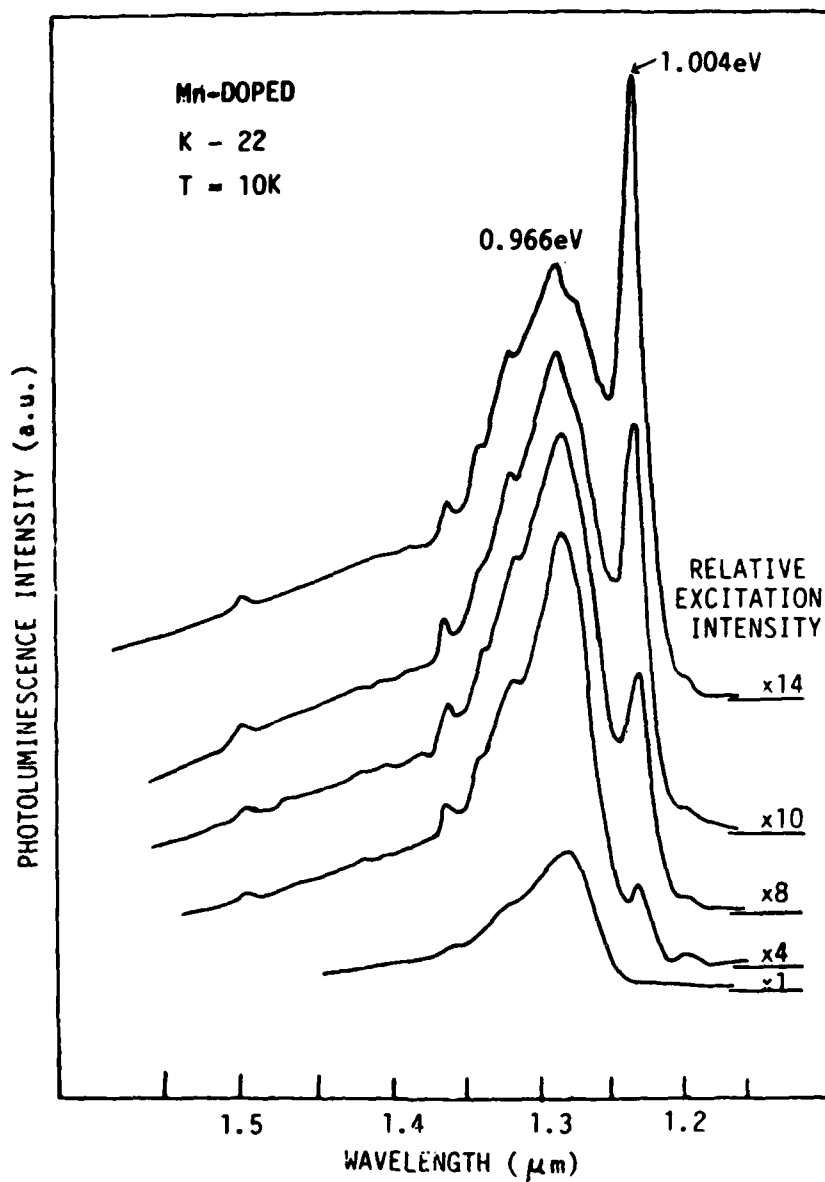of the PL peak energy in the undoped sample.

42

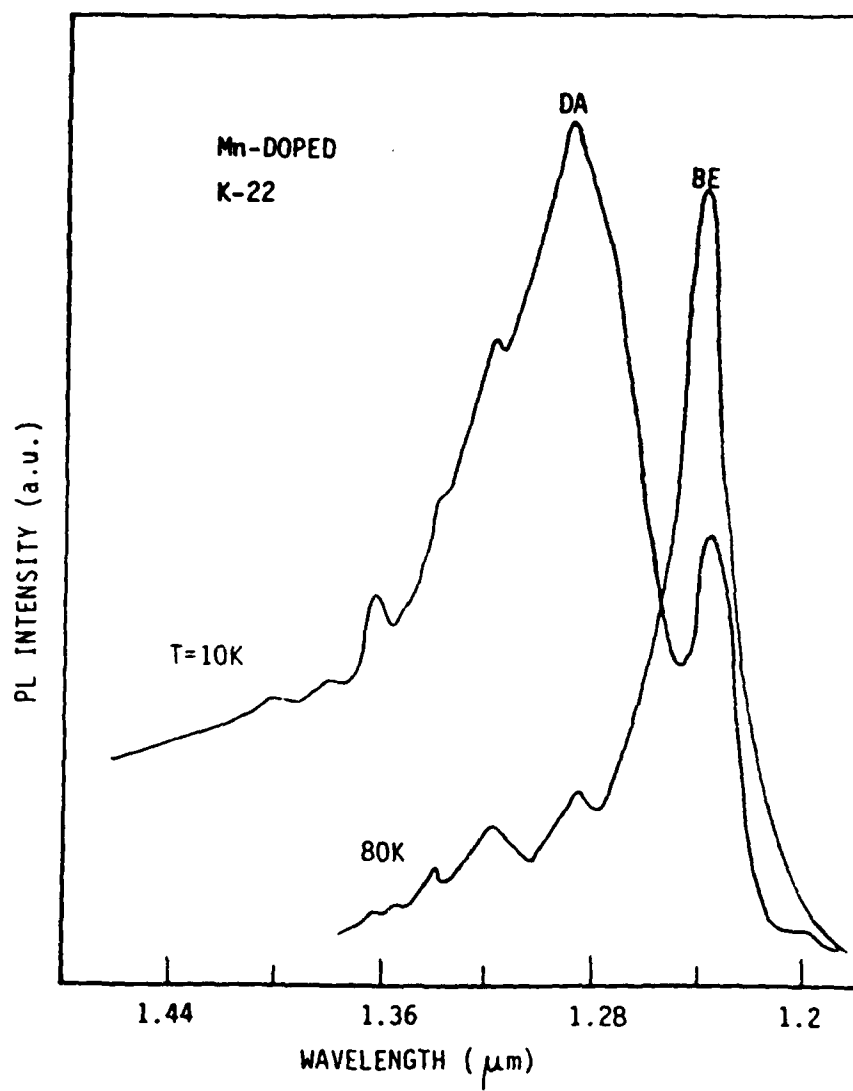Figure 7. Photoluminescence of Mn-doped sample K-22, as a function of incident excitation level.

43

Figure 8. PL spectra of Mn-doped sample K-22 as a function of temperature.

44

CHARACTERIZATION OF Mn-DOPED $In_{1-x}Ga_xAs_yP_{1-y}$ GROWN BY LPEE

SHANTHI N. IYER, ALI ABUL-FADL, WARD J. COLLIS AND MOHAMMAD N. KHORRAMI
North Carolina A & T State University, Greensboro, NC 27411

ABSTRACT

Mn-doped $In_{1-x}Ga_xAs_yP_{1-y}$ epilayers lattice matched to InP substrate have been grown by the liquid phase electroepitaxial (LPEE) technique. The variation of growth velocity of the epilayers with current density and the doping characteristics of Mn in the epilayer has been studied. The temperature dependence of the hole concentration and the mobility has been analysed to determine the donor and acceptor densities, thermal activation energy of the level associated with Mn and the dominant scattering mechanisms that limit the hole mobility. The photoluminescence spectra of the doped epilayers are examined at 10K as a function of the excitation level.

INTRODUCTION

$In_{1-x}Ga_xAs_YP_{1-y}$ quaternary alloys lattice matched to InP are one of the most extensively studied III-V alloy system. Different techniques have been employed for the growth of these layers. In our earlier work [1] we have reported the growth of the quaternary layers by the liquid phase electroepitaxial (LPEE, also known as current controlled liquid phase epitaxy) technique. LPEE has the advantage that as the growth is controlled by an external parameter (electric current), uniformity in epilayer thickness and composition [2,3], interface stability [4] and the epilayer surface morphology [5] are better than those grown by the conventional LPE techniques. Further, this technique provides limited control on the dopant segregation [6] and the defect structure [7].

In this paper, we report the growth of Mn-doped $In_{1-x}Ga_xAs_yP_{1-y}$ layers by the LPEE technique. Mn was chosen as it has been found [8-10] to be a suitable p-type dopant for device applications, in quaternary alloys of compositions closer to the ternary $In_{.53}Ga_{.47}As$. The hole concentration and the hole mobility were investigated, in detail, to estimate the activation energy of the dopant, carrier compensation and the prevalent scattering mechanisms in the quaternary and are compared with the published data. We have also examined the band-edge luminescence in these layers at 10K as a function of excitation intensity.

EXPERIMENTAL

The growth method utilizes the conventional horizontal slider boat system modified to permit the passage of electric current through the substrate-melt

interface. The details of the growth system, source materials used and the substrate preparations have been described earlier [1,11]. Semi-insulating (100)-oriented InP wafers of 0.4 mm (16 mil) thickness and 1x1 cm in area were used as the substrates. Elemental 4N purity Mn was used as the source material for Mn concentrations in the melt exceeding 10^{-3}. For lower concentrations Mn diluted with In and baked at 740°C for homogenization, was used as the dopant source.

RESULTS AND DISCUSSION

Growth velocity and doping characteristics

The growth velocity of the Mn-doped quaternary epilayers, corresponding to the composition of x = 0.29 and y = 0.64, was studied as a function of current density ranging from 3 A/cm^2 to 8 A/cm^2. Though there is a lot of scatter in the data, as shown in Fig.1, the growth velocity seems to increase linearly with current density indicating electromigration to be the dominant mechanism contributing to the growth process. The growth velocity of the Mn-doped quaternary layer is typically 6-7 µm/hr at a current density of 5 A/cm^2.

Our results on the doping characteristics of the Mn-doped layer along with that of Fujita et al. [8] is shown in Fig.2. The Hall measurement carried out on undoped quaternary layer indicated a residual doping level of $10^{16}/cm^3$ in these layers. The hole concentration in the doped layers is found to vary as $(X_{Mn}^{\ell})^n$, the value of n being 0.32 at doping levels below 10^{-3} and 0.7 at higher doping concentrations. The highest hole concentration we have obtained in these layers is $\sim 4 \times 10^{18}/cm^3$. Attempts to grow these layers from the melts with X_{Mn}^{ℓ} above 10^{-2} resulted in poor quality epilayers with melt sitting on top of the substrate after growth termination. A similar effect was also observed
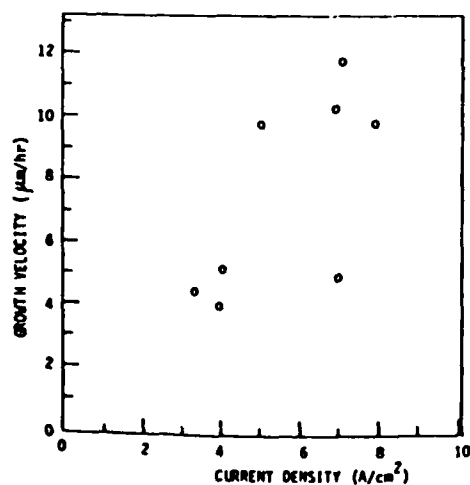
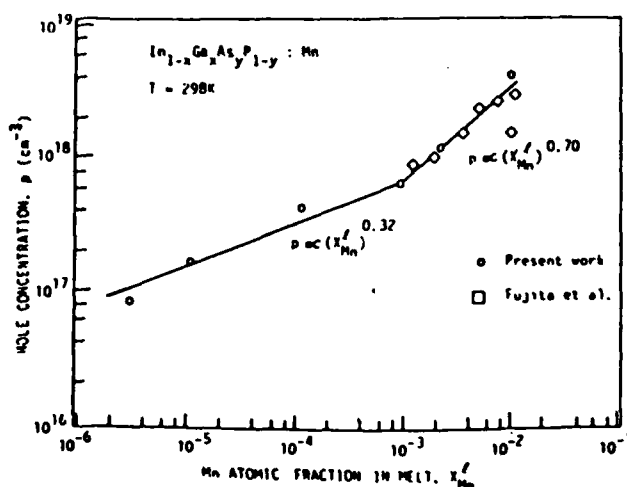Fig.1. Dependence of growth velocity on current density

Fig.2. Variation of hole concentration with Mn concentration in the melt.

by Whitney et al. [12] on Mn-doped $In_{0.53}Ga_{0.47}As$, indicating that it is the solid solubility of Mn in the quaternary layer that imposes the limit on the carrier concentration obtained in these layers.

Both the undoped·and doped layers exhibit a large positive mismatch of ~0.2%. However, the surface morphology was excellent (mirror smooth) even up to a Mn concentration of $2x10^{-3}$. Further, the fine terracing that is commonly observed in the LPEE grown undoped layers was absent. Layers of 20 μm thickness with good surface morphology have been grown by this technique. The layer thickness for our study ranged from 4 μm to 10 μm.

Electrical properties

Figure 3 illustrates the dependence of Hall mobility measured at room temperature and at 77K on room temperature hole concentration. Published data points [8,9] for Mn-doped quaternary are also included for comparison. The values of mobilities we have obtained are a little higher than the reported values for the layers grown by conventional LPE. The variation of hole concentration with temperature in the range of 60K - 300K is shown in Fig.4. Unity Hall scattering factor was assumed in the computation of carrier concentration in the temperature range investigated. The data were analysed using the expression for carrier concentration in non degenerate semiconductors, where the acceptor activation energy (E_A), donor (N_D) and acceptor (E_A) densities were treated as the fitting parameters. The values of these parameters that resulted in a best fit with the linear portion of the experimental data are listed in Table 1. The activation energy of the acceptor level
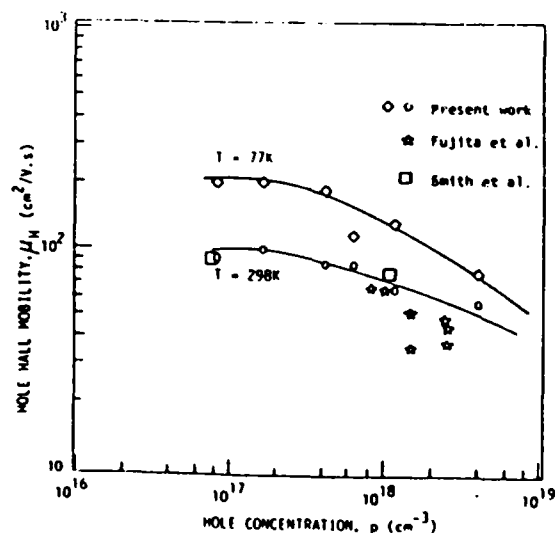

Fig.3. Liquid nitrogen and RT hole mobility as a function of RT hole concentration.
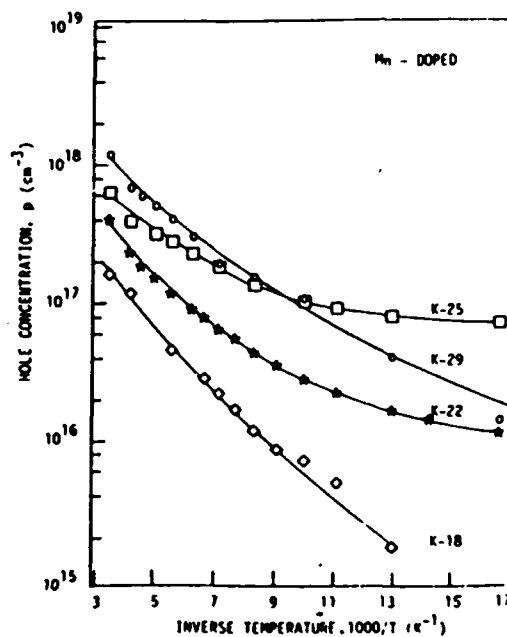
Fig.4. Temperature dependence of hole concentration.

TABLE 1. Electrical properties of Mn-doped quaternary layers

Sample No.	p (cm^{-3})	E_A(meV)	$N_A(cm^{-3})$	$N_D(cm^{-3})$	$N_A^*(cm^{-3})$	$N_D^*(cm^{-3})$
K-18	1.6×10^{17}	57	3×10^{17}	4×10^{16}	7×10^{17}	4×10^{17}
K-22	4.1×10^{17}	45	4.5×10^{17}	3×10^{16}	9×10^{17}	4.5×10^{17}
K-25	6.3×10^{17}	32	8.5×10^{17}	4.5×10^{16}	2.2×10^{18}	1.2×10^{18}
K-29	1.2×10^{18}	32	3×10^{18}	5×10^{17}	-	-

decreases from 57 meV to 32 meV with increasing hole concentration. The computed value of donor to acceptor ratio is low ranging from 0.05 to 0.2.

The acceptor and donor concentrations were also estimated from the temperature variation of Hall mobility (Fig.5). Contributions due to polar optical phonon scattering, ionized impurity scattering, alloy scattering, non-polar optical phonon and acoustic scattering were taken into account using Matheissen's rule. The equations used in the analysis of scattering mechanisms are given in Ref.13 and the parameters used in the computation of the hole mobility are listed in Table 2. These parameters have been estimated from the linear interpolation of the values from the binary constituents [13]. N_D, N_A and alloy scattering potential (ΔU_p) were the adjustable parameters. A good fit to the experimental data (Fig.6) has been obtained for $\Delta U_p = 0.2$, which is close to the value determined by Hayes et al. [13]. The values of N_D^* and N_A^* determined from the mobility data (listed in Table 1) are much larger than the corresponding values estimated from the temperature dependence of the concentration data. The large discrepancy between these two values could be attributed to any one or combination of the following. (a) The absence of strong freeze out in these layers suggest the impurity banding, which makes the estimated values from both the analysis inaccurate, with the mobility data tending to overestimate the values of N_D^* and N_A^*. (b) The computation of the ionized impurity scattering using Brooks -Herring formula at these high doping levels could have significant effect in the calculated mobility values. In fact, a good fit could not be obtained for sample K-29 which has a room temperature carrier concentration of $1.2 \times 10^{18}/cm^3$. However, the analysis of both the mobility and Hall constant data indicate somewhat lower compensation in these layers than normally observed in p-layers using the other dopants [14,15].
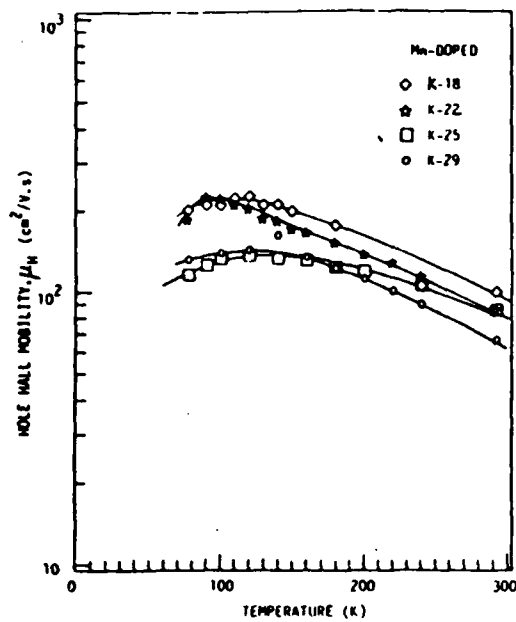
Fig.5. Temperature dependence of hole mobility for Mn-doped quaternary layers
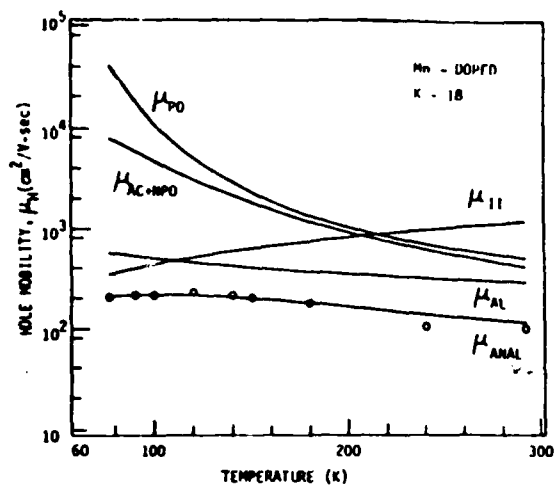

Fig.6. Temperature variation of hole mobility in sample K-18. The solid line through the data points is the computed value of the mobility taking into account the different scattering mechanisms.

Photoluminescence

Photoluminescence spectra of the Mn-doped quaternary sample at 10K with a doping level of $4x10^{17}/cm^3$ is shown in Fig.7 for different excitation levels. The spectra of these samples are characterized by two peaks, a sharp peak at 1.004 eV which is related to the near band edge emission (BB) in undoped sample and a broader peak displaced towards lower energies. The saturation of broad band peak at higher intensity in conjunction with the dominance of BB peak indicates that the broad band peak is related to donor-Mn acceptor (DA) level. The difference between these two peak energy values (~38 meV) is in good agreement with the value of the thermal activation energy of Mn level determined from the Hall data. For layers with higher doping levels, saturation of DA photoluminescence intensity occurs at higher excitation levels as expected.

CONCLUSION

Mn-doped $In_{1-x}Ga_xAs_yP_{1-y}$ epilayers of good surface morphology have been grown by the LPEE technique. The growth velocity of these layers is typically ~6.5 µm/hr at a current density of 5 A/cm^2. Hole concentration between $8x10^{16}/cm^3$ and $4x10^{18}/cm^3$ with room temperature Hall mobilities ranging from 98 to 56 cm^2/V.s have been obtained in these layers. The activation energy of the Mn acceptor level decreased from 57 meV to 32 meV with increasing hole

49

TABLE 2. The values of the physical parameters used in the computation of analytical hole mobility

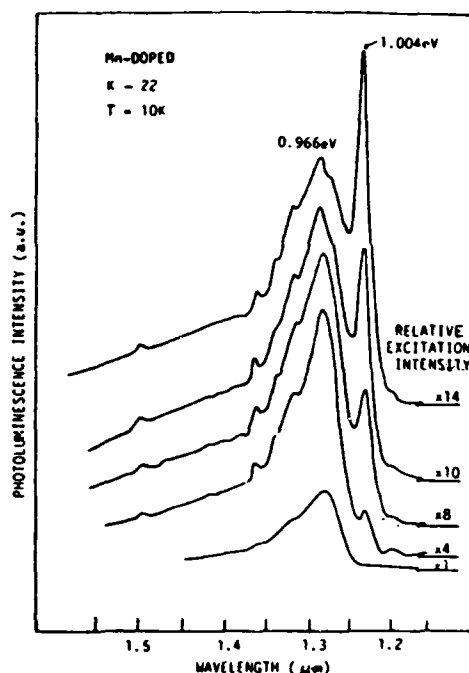| Parameter	Value
e^*/e	0.23
m_ℓ^*/m_0	0.064
m_h^*/m_0	0.687
θ (K)	426
E_{AC} (eV)	3.389
E_{NPO} (eV)	6.107

Fig.7. Variation of photoluminescence intensity with excitation level

concentration from $1\times10^{17}/cm^3$ to $1.2\times10^{18}/cm^3$. The values of the acceptor and donor densities determined from the Hall mobility data are consistently higher than the respective values determined from the Hall constant data. This may be related to either or both the inadequacy of Brooks-Herring formula for the computation of ionized impurity scattering at these high doping levels and the presence of the impurity band conduction. The optical activation energy of Mn level as determined from the photoluminescence measurements is in good agreement with the value of the thermal activation energy.

ACKNOWLEDGEMENTS

REFERENCES

1. S. Iyer, E.K. Stefanakos, A. Abul-Fadl and W.J. Collis, J. Cryst. Growth 70, 162 (1985).

2. L. Jastrzebski, Y. Imamura and H.C. Gatos, J. Electrochem. Soc. 125, 1140 (1978).

3. J.J. Daniele and A. Lewis, J. Electron. Mater. 12, 1015 (1983).

4. A. Okamoto, J. Lagowski and H.C. Gatos, J. Appl. Phys. 53, 1706 (1982).

5. Y. Imamura, L. Jastrzebski and H.C. Gatos, J. Electrochem. Soc. 125, 1560 (1978).

6. J. Lagowski, L. Jastrzebski and H.C. Gatos, J. Appl. Phys. 51, 364 (1980).

7. Y. Imamura, L. Jastrzebski and H.C. Gatos, J. Electrochem. Soc. 123, 1381 (1979).

8. S. Fujita, M. Kuzuhara, M. Yagyu and A. Sasaki, Solid State Electron. 25, 359 (1982).

9. A.W. Smith. L.G. Shantharama, L. Eaves, P.D. Greene, J.R. Hayes and A.R. Adams, J. Phys. D : Appl. Phys. 16, 679 (1983).

10. Y. Takeda, M. Kondo, N. Okano and A. Sasaki, Solid State Electron. 29, 241 (1985).

11. A. Abul-Fadl, E.K.Stefanakos and W.J. Collis, J. Electron. Mater. 11, 559 (1982).

12. P.S. Whitney and C.G. Fonstad, J. Appl. Phys. 57, 4663 (1985).

13. J.R. Hayes, A.R. Adams and P.D. Greene, in GaInAsP Alloy Semiconductors, edited by T.P. Pearsall (Wiley, New York, 1982), p. 189; J. Electron. Mater. 11, 155 (1982).

14. Mulpuri V. Rao, J. Appl. Phys. 58, 4313, (1985).

15. T.P. Pearsall, G. Beuchet, J.P. Hirtz, M. Visentin, M. Bonnet and A. Roizes , Proc. of the Eighth International Symposium on Gallium Arsenide and Related Compounds, Vienna, 1980 (Inst. of Phys., Bristol) p.639.

SELECTIVE ELECTROEPITAXIAL GROWTH OF $In_{0.53}Ga_{0.47}As$
ON (100) - Fe:InP

ALI ABUL-FADL, SAMIR MAANAKI, WARD COLLIS and SHANTHI IYER

North Carolina A&T State University
Department of Electrical Engineering
Greensboro, North Carolina 27411

Abstract

Electroepitaxy has been used to grow InGaAs on
selected (100) InP islands using a sputtered
SiO_2 layer as the substrate mask. The epitaxial
layers were characterized with respect to their
surface morphology and thickness uniformity.
The electric field intensity along the substrate
melt (S-M) interface of the islands is found by
solving the field equation by the finite element
method. Experimental results show that the
uniformity of the grown islands can be directly
related to the uniformity of the electric field
along the S-M interface.

Introduction

Studies on selective epitaxial growth within
windows and on etched substrates have been
reported by several investigators [1-10]. The
interest in the selective epitaxial growth into
the window opening of a mask lies with the
inherent capability of establishing isolated
areas of epitaxial regions. These regions have
the potential to realize two- and three-dimension-
al devices for the fabrication of optoelectronic
integrated circuits. Several growth techniques
have been used to grow selectively on InP [1-5]
and GaAs [6-10] substrates, since these materials
are the basis for many semiconductor devices
employed in glass-fiber communication systems for
the wave length ranges from 1.2 to 1.6µm and 0.85
to 1.1µm. The growth techniques include liquid
phase epitaxy (LPE) [1-4], LPE electroepitaxy
(LPEE) [5], organometalic chemical vapor deposit-
ion (OMCVD) [7], vapor phase epitaxy (VPE) [8]
and molecular beam epitaxy (MBE) [9,10].

This study was undertaken to investigate the
growth morphology of layers of InGaAs grown
selectively on SiO_2-masked Fe-doped InP substrates.
The growth was performed by electroepitaxy (LPEE)
at a constant furnace temperature by passing a
direct electric current from the substrate to the
melt.

A mathematical model of electroepitaxy was also
developed and a solution for Poisson's equation
in the substrate and along the substrate-melt
interface was obtained using the finite element
method.

Experimental Procedure

The selective growth of InGaAs was carried out in
a modified LPE apparatus with a sliding graphite
boat, described elsewhere [11]. The samples used
in this study were (100) semi-insulating (iron-
doped) InP substrates (12 x 12mm and about 400µm
thick). They were cleaned with organic solvents
using warm trichloroethylene (TCE), acetone and
methanol. The masking pattern was first formed in
a photoresist layer. A sputter deposited SiO_2 layer
(1000 - 2800 Å) was then applied to the exposed
areas and finally the photoresist was removed by
acetone, leaving behind the SiO_2 mask. The InP
islands defined by the SiO_2 mask were of various
sizes (80 x 1000µm to 3000^2 x 3000µm) and different
geometries (narrow and wide strips, square, circular)
The patterned substrate was then cleaned with
organic solvents and stir etched with a 1% Br-
methanol before it was loaded into the growth boat.

The growth was performed at a constant furnace
temperature of 640°C by passing a direct electric
current of $1 A/cm^2$ for a period of 15 minutes.
Although the semi-insulating substrates have a room
temperature resistivity exceeding $10^7 \Omega$-cm, at the
growth temperature (640°C) the conductivity is
adequate for LPEE to be performed. At this temper-
ature, the intrinsic carrier concentration is about
$5 \times 10^{16}/cm^3$. In addition, it is also possible that
deep impurity levels in the semi-insulating sub-
strate are ionized, tending to increase the conduct-
ivity further. Experimental measurements of the
substrate resistance at the growth temperature
resulted in about 60 mΩ.

After growth the substrate was removed from the
growth apparatus and the layer was examined by
interference contrast microscopy. The morphology
and uniformity of the layers were studied by cleav-
ing and etching several samples with $K_3Fe(CN)_6$:KOH:
H_2O solution to delineate the growth layer from the
substrate.

Experimental Results

Typical surface morphology of the selectively grown
layers are shown in figures 1, 2, and 3. Figures
1 and 2 are photomicrographs of a narrow strip
(150 x 1000µm) and a circular area with a radius of
250µm respectively. Figure 3 is a photomicrograph
of a wide strip (780 x 2000µm). Figures 1 and 2
clearly show terrace-free surfaces with no voids or
defects or other features. In figure 3 the surface
morphology is similar to those in figures 1 and 2

52

except for the central region where the layer is about 3.7μm thinner and of inferior quality. The abnormal growth in the central region of the wide strip geometries is attributed to non-uniformity of the electric field.
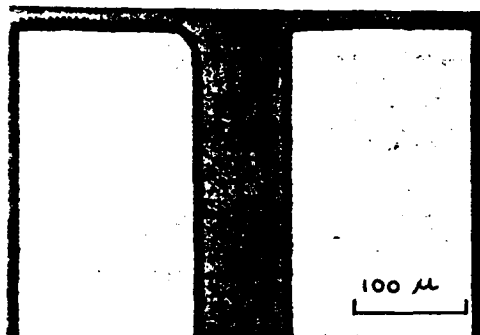

Figure 1. Surface morphology of InGaAs epilayer grown on a narrow strip geometry at 640°C and 1A/cm²-15 minutes.

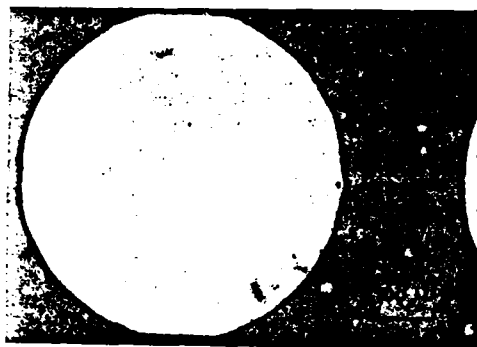Figure 2. Surface morphology of InGaAs epilayer grown on a circular geometry at 640°C and 1A for 15 minutes.
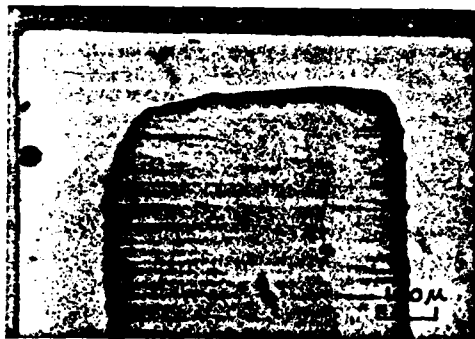

Figure 3. Surface morphology of InGaAs epilayer grown on a wide strip geometry at 640°C and 1A for 15 minutes.

Figure 4 is a photomicrograph of a cleaved section of the layer shown in figure 1. The figure shows a 1.2μm etched layer from the substrate and the grown layer. The shape of the growth layer that protruded from the substrate coincided with the mask pattern and the sides of the layer are perpendicular to the <111> directions (about 54.8° angle with the (100) surface).

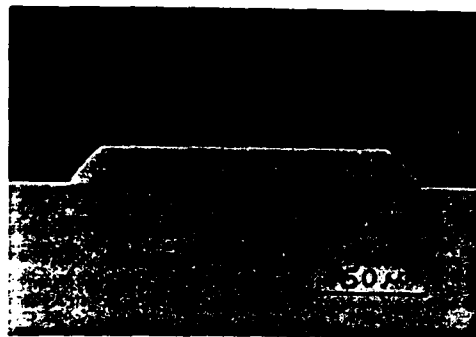Figure 4. Cleaved section of the narrow strip shown in Fig. 1. The layer is about 17μm thick and 150μm wide.

Figure 5 shown two narrow strips, side-by-side. The strips are about 80μm wide and about twice as thick as the layer shown in figure 4. The shape of the cross-section is trapezoidal and the side walls are determined to be (111) planes. The photographs also show that the layer-substrate interface is smooth in all cleaved sections and all undercutting by the chemical etching of the substrate is completely filled with the growth layer.
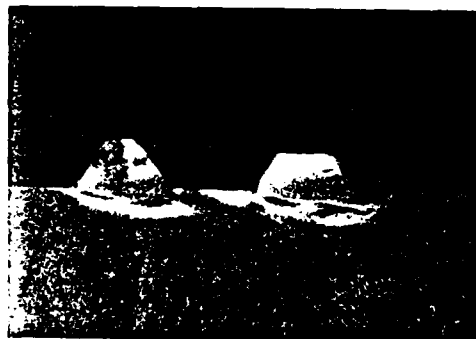

Figure 5. Cleaved section of two narrow strips side-by-side. The one strip is about 80μm wide and 45μm thick and the other strip is about 100μm wide and 34μm thick.

Electroepitaxy model

In the mathematical model of selective electro-epitaxy presented in this study it is assumed that the solute transported to the advancing growth interface is removed from the solution only through

53

epitaxial growth on the substrate. The theoretical model developed by Bryskiewicz [12] for LPEE of multicomponent systems yields the following expression for the growth velocity

$$V = -\Delta T_0 f_1 + E f_2$$

where ΔT_0 is the change in interface temperature, primarily due to the Peltier cooling at the semiconductor-melt (S-M) interface, E is the electric field due to the electric current flow, f_1 and f_2 are functions of melt components and are independent of ΔT_0 and E. Under low current conditions and thin substrates, the interaction between the Peltier cooling on one side and the Peltier heating on the other side of the substrate is high (ΔT_0 can be neglected) and the growth is primarily due to the electric field E such as

$$V = E f_2$$

The above equation indicates that under controlled conditions, the layer uniformity is governed by the uniformity of the electric field along the S-M interface. To solve for the electric field, a mathematical model shown in figure 6 with the applied boundary conditions is used. The electric field is considered within the substrate bounded by the back contact melt on one side and the growth melt on the other side. The growth melt side is non-receptive for crystal growth except for a strip-like region of width w. A two dimensional Poisson's equation is considered for the mathematical analysis to solve for the electric field distribution in the substrate and along the substrate-melt interface.

MELT - InP
$\phi(x,d) = 0$
$\frac{\partial\phi}{\partial y}\big|_{0,d} = 0$

SiO$_2$ - InP
$\phi(w,d) = 0.94$
$\frac{\partial\phi}{\partial y}\big|_{InP} = \frac{\varepsilon_i}{\varepsilon_s}\frac{\partial\phi}{\partial y}\big|_{SiO_2}$

$\nabla^2\phi = \rho_s/\varepsilon_s$

InP

W,

MELT - InP
$\phi(x,o) = C_1$
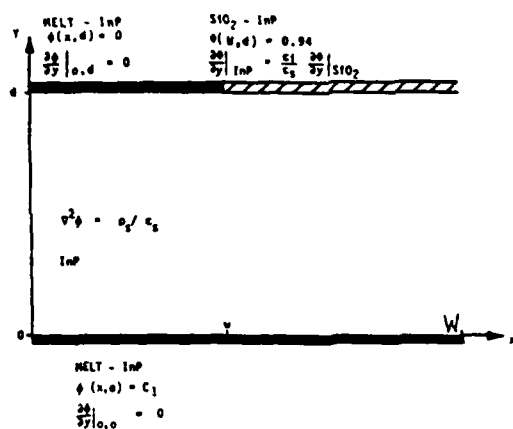$\frac{\partial\phi}{\partial y}\big|_{0,0} = 0$

Figure 6. Schematic cross-section of the substrate, growth melt, and back contact melt, model used to analyze selective epitaxy.

The equation in two dimension is of the form

$$\frac{\partial^2\phi}{\partial x^2} + \frac{\partial^2\phi}{\partial y^2} = -\frac{\rho_s}{\varepsilon_s}$$

where ϕ, ρ_s, ε_s, are the electric potential total space-charge in the semiconductor and permittivity of the semiconductor respectively. The model is divided into three regions for the applied boundary conditions the back contact melt-InP region the growth melt-InP region, and the SiO$_2$-InP region.

The electric field $\frac{\partial\phi}{\partial y}$ in the growth melt at $y \geq d$ and back contact melt $y \leq 0$ is

$$\frac{\partial\phi}{\partial y} = \frac{J}{\sigma}$$

where J is the electric current density and σ is the conductivity of the melt. If one assumes an ideal metal (the In melt), σ is very large and for small current density $\frac{\partial\phi}{\partial y}$ is approximately equal to zero. At the SiO$_2$-InP interface, the electric field is proportional to the ratio of permittivities such as

$$\frac{\partial\phi}{\partial y}\Big|_{InP-SiO_2} = \frac{\varepsilon_i}{\varepsilon_s}\frac{\partial\phi}{\partial y}\Big|_{SiO_2}$$

where ε_i is the insulator permittivity and ε_s is the InP permittivity. For $\phi(x,0) = 1.0$ volt and an oxide thickness of 2800 Å, $\frac{\partial\phi}{\partial y}\big|_{SiO_2}$ is approximately equal to 3.57 V/µm and $\frac{\partial\phi}{\partial y}\big|_{InP-SiO_2}$ is calculated to be about 1.12V/µm. The electric potential along the substrate-growth-melt interface is set to 0.0 volt, and at $x = W$, $y = d$, $\phi(W,d) = \phi(x,0) - I R_{sub}$. For $I = 1.0A$ and $R_{sub} = 60$ mΩ $\phi(W,d)$ is about 0.94 V.

The total space-charge ρ_s in the substrate is given by

$$\rho_s = -q(n-p + N_D^*)$$

where q, n, p, and N_D^* are the elementary charge, electron density, hole density, and ionized impurities from deep levels, respectively. Since $n = p = n_i$ at the growth temperature (640°C), then

$$\rho_s = -qN_D^*$$

where N_D^* range from over $6 \times 10^{15}/cm^3$ to nearly $4 \times 10^{16}/cm^3$.

A finite element method is applied to the solution of Poisson's equation over the defined model. The equipotential and field cantour plots for narrow strip and wide strip geometries are shown in figures 7 and 8.
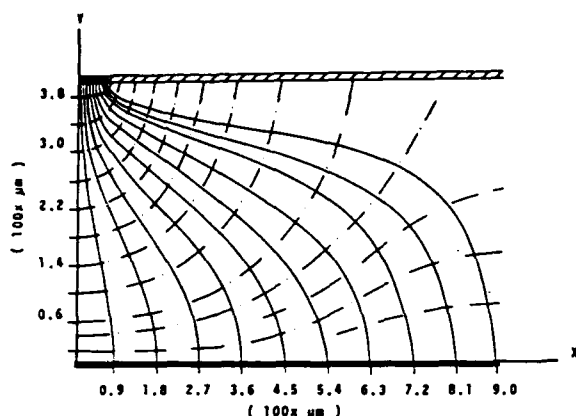
Figure 7. Equipotential and electric-field
contour plots for narrow strip geometry
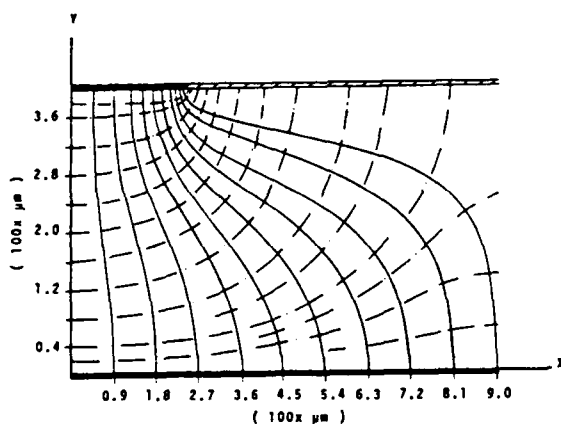($\frac{1}{2}$ section).

Figure 8. Equipotential and electric field
cont ur plots for wide strip geometry
($\frac{1}{2}$ section).

Plots of the normalized field intensity along the
growth melt-substrate interface for the two
geometries is shown in figure 9. The field
intensity is calculated using the equipotential
contour plot closest to the strip and a grid
increment of 20μm wide. The plots clearly show
that the field intensity along narrow strip
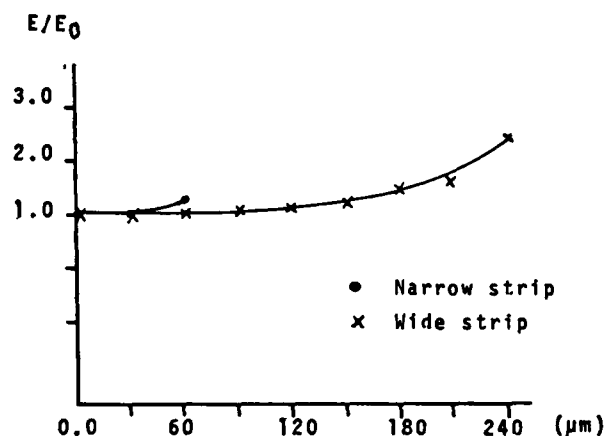geometry is more uniform than in wide geometry.

Figure 9. Normalized electric field intensity
plots for narrow and wide geometries.

Conclusion

The computer simulation results show that the
electric field intensity along the growth interface
for narrow strip geometry is more uniform than in
wide geometry. As a result, the layer grown on
narrow strips were more uniform and have better
surface morphology.

Acknowledgements

References

1. S.E.H. Tuffly and P.D. Green, J. Cryst. Growth
   58, 409 (1982).
2. N. Chand and P. A. Houston, J. Elect. Mater.
   14, 9 (1985).
3. N Chand, A. V. Syrbu and P. A. Houston,
   J. Cryst. Growth, 61, 53 (1983).
4. F. Fiedler and A. Schlachetzki, J. Cryst.
   Growth, 53 623 (1981).
5. R.D. Feldman, and R. F. Austin, J. Cryst.
   Growth, 71, 1   (1985).
6. X. F. Yang, L. Huang and H. C. Gatos, J. Electro
   chem. Soc. 130, 1381 (1983).
7. K. Okamoto and K. Yamaguchi, Appl. Phys. Lett.
   48, 849 (1986).
8. N. Vodjdjani, M. Erman and J.B. Theeten,
   J. Cryst. Growth, 71,   141 (1985).
9. J.M. Hong, S. Wang, T. Sands, J. Washburn,
   J.D. Flood, J. J. Merz and T. Low, Appl. Phys.
   Lett. 48, 142 (1986).
10. T. Venkatesan and B. Wilkeens, Appl. Phys. Lett.
    48, 145 (1986).
11. A. Abul-Fadl, E.K. Stefanakos and W.J. Collis,
    J. Elect. Mater. 11, 559 (1982).

12. T. Bryskiewicz, J. Lagowski and H.C. Gatos,
    J. Appl. Phys. 51, 988 (1980).

APPENDIX C

Presentations

"Selective Electroepitaxial Growth of $In_{0.53}Ga_{0.47}As$ on (100)-Fe:InP",
1987 SOUTHEASTCON, Tampa Florida. April 5-8, (1987).

"Selective Etch-back and Growth of $In_{0.53}Ga_{0.47}As$ on (100) Fe:InP by
Electroepitaxy", 1987 Elect. Mater. Nonf., Santa Barbara, Calif., June 5-8, (1987).

"Properties of Undoped and Mn-doped InGaAsP Grown by Liquid
Phase Electroepitaxy", 7th International Conf. on Thin Films, New Delhi,
India, December 7-11, (1987)

SELECTIVE ELECTROEPITAXIAL GROWTH OF $In_{0.53}Ga_{0.47}As$ ON (100) - Fe:InP

By

A. Abul-Fadl, S. Maanaki, W. Collis and S. Iyer
North Carolina A&T State University
Department of Electrical Engineering
Greensboro, North Carolina 27411

ABSTRACT

Electroepitaxy has been used to grow InGaAs on selected (100) InP islands using a sputtered SiO_2 layer as the substrate mask. The epitaxial layers were characterized with respect to their surface morphology and thickness uniformity. The electric field intensity along the substrate-melt (S-M) interface of the islands is found by solving the field equation by the finite element method. Experimental results show that the uniformity of the grown islands can be directly related to the uniformity of the electric field along the S-M interface.

SELECTIVE ETCH-BACK AND GROWTH OF $In_{0.53}Ga_{0.47}As$ ON (100) Fe:InP BY ELECTROEPITAXY

By

Ali Abul-Fadl, Ward Collis, Samir Maanaki, Taunya McCarty
and Shanthi Iyer
North Carolina A&T State University
Greensboro, N.C. 27411

Selective etch-back prior to growth of InGaAs islands on SiO_2-masked (100) Fe-doped InP substrates was performed by electroepitaxy. The etch-back of the substrate and the growth of the layer was done at a constant furnace temperature of 640°C by passing a direct electric current from the melt to the substrate for etch-back and from the substrate to the melt for growth. The current density used was 1 to $5A/cm^2$ for a period of 15 minutes. The isolated InP regions were of various sizes (80 x 1000μm to 3000 x 3000μm), and different geometries (narrow and wide strips, square, circular). A uniform etch-back and uniform growth with excellent surface morphology (no terraces or voids or defects) was obtained on strips as wide as 200μm and on circles with d < 500μm. For islands with wider geometry, the etch-back was not as uniform and the growth was uniform up to 100 - 200μm from the periphery with excellent surface morphology. However, the central region was slightly thinner and the surface morphology was of inferior quality.

The uniformity of etch-back as well as the growth of different geometries is attributed to the uniformity of the electric field along the substrate melt interface (S-M). A mathematical model is used to investigate the uniformity of the field along the S-M interface. Numerical solution to the field equation for different geometries is done by the finite element method.

The etch-back and growth results will be presented. Also the computer simulation results of the model for different geometries will be presented and an attempt will be made to explain the uniformity or non-uniformity of the various islands grown by this technique.

PROPERTIES OF UNDOPED AND MANGANESE-DOPED InGaAsP GROWN BY LIQUID PHASE ELECTROEPITAXY*

SHANTHI N. IYER, ALI ABUL-FADL, WARD J. COLLIS AND MOHAMMAD N. KHORRAMI

North Carolina A&T State University, Greensboro, NC (U.S.A.)

Undoped and manganese-doped InGaAsP epilayers lattice matched to InP substrate have been grown by the liquid phase electroepitaxy technique. The dependence of growth velocity on current density for both undoped and doped layers has been studied. Layers of good surface morphology with hole concentrations in the range from 8×10^{16} to 4×10^{18} cm^{-3} have been achieved. The activation energy of the manganese acceptor level was estimated to vary from 57 to 32 meV with increasing hole concentration. The temperature dependence of carrier mobility data was analyzed in terms of different scattering mechanisms and the values of acceptor and donor densities determined were compared with those obtained from the temperature variation of Hall concentration data. Dependences of photoluminescence peak energy and intensity on the temperature and incident excitation levels have been investigated.

1. INTRODUCTION

Liquid phase epitaxy has been one of the extensively used and preferred growth technique for InGaAsP compounds. The liquid phase electroepitaxy (LPEE) technique differs from the conventional liquid phase epitaxy technique in that the growth is primarily controlled by the current density passing through the melt–substrate interface at the liquidus temperature. As the growth is carried out at a constant furnace temperature, this technique facilitates better control on the thickness[1] and doping of the layer[2]. Further, it has been shown that layers grown by this technique exhibit better compositional homogeneity[3,4] with improved interface stability[5] and surface morphology[6].

In our previous paper[7], we have reported the growth of an InGaAsP layer lattice matched to InP by the LPEE technique in the entire composition range of the quaternary alloy. However, thick layers of good quality (surface morphology) were difficult to grow for compositions in the middle of the alloy range, which was attributed to the presence of the miscibility gap. This problem has been circumvented by raising the growth temperature to 685 °C as suggested by Schemmel *et al.*[8], where a stable composition can be grown.